

10738 4634 NACA
NACA TN 4394 83701

TECH LIBRARY KAFB, NM
0067198

NATIONAL ADVISORY COMMITTEE FOR AERONAUTICS

TECHNICAL NOTE 4394

THE RATE OF FATIGUE-CRACK PROPAGATION IN
TWO ALUMINUM ALLOYS

By Arthur J. McEvily, Jr., and Walter Illg

Langley Aeronautical Laboratory
Langley Field, Va.



Washington
September 1958

AEMDC
TECHNICAL LIBRARY



NATIONAL ADVISORY COMMITTEE FOR AERONAUTICS

TECHNICAL NOTE 4394

THE RATE OF FATIGUE-CRACK PROPAGATION IN
TWO ALUMINUM ALLOYS

By Arthur J. McEvily, Jr., and Walter Illg

SUMMARY

A general method has been developed for the determination of fatigue-crack propagation rates. In order to provide a check on the theoretical predictions and to evaluate certain empirical constants appearing in the expression for the rate of fatigue-crack propagation, an extensive series of tests has been conducted. Sheet specimens, 2 inches and 12 inches wide, of 2024-T3 and 7075-T6 aluminum alloys were tested in repeated tension with constant-amplitude loading. Stresses ranged up to 50 ksi, based on the initial area. Good agreement between the results and predictions was found.

INTRODUCTION

The rate of propagation of fatigue cracks is a subject not only of academic but also of practical interest as applied to fail-safe design. Some theoretical and experimental work has already been done in this field, but as yet no generally applicable method for the quantitative prediction of the rate of fatigue-crack propagation is available. The aim of the present investigation is to present such a method and apply it to the aluminum alloys 2024-T3 and 7075-T6.

SYMBOLS

a	semimajor axis of ellipse, in.
c	half-width of plate, in.
C_1	material constant, ksi
C	constant of integration, cycles

f, f_1, f_2	rate-determining functions
K_E	theoretical stress-concentration factor for ellipse
K_H	theoretical stress-concentration factor for circular hole
K_N	theoretical stress-concentration factor modified for size effect
K_T	theoretical stress-concentration factor
n	exponent
N	number of cycles
ΔN	incremental number of cycles
r	rate of fatigue-crack propagation, in./cycles
R	ratio of minimum stress to maximum stress
S_e	endurance limit (or the stress at 10^8 cycles), ksi
S_{net}	maximum load divided by remaining net sectional area, ksi
S_o	maximum load divided by initial net sectional area, ksi
x	one-half of total length of central symmetrical crack, in.
α	stress-dependent proportionality constant, in. $^{-\frac{1}{2}}$ /cycle
η	number of cycles from beginning of work-hardening stage
ρ	radius of curvature, in.
ρ'	Neuber material constant, in.
ρ_e	effective radius of curvature at tip of fatigue crack, in.
σ	local stress, ksi
σ_f	fracture strength of critical region, ksi
σ_y	yield strength of critical region, ksi

THEORETICAL CONSIDERATIONS

Background Information

An excellent review of the state of knowledge on the growth of fatigue cracks has recently been given by Schijve (ref. 1) and will not be repeated in detail herein. However, the work of Head (ref. 2) and Weibull (refs. 3, 4, and 5) is of particular interest and will be briefly described.

Head developed a physical model of the process of fatigue-crack propagation based upon Orowan's concept of fatigue (ref. 6), which considers that localized fracture occurs as the result of an increase in stress due to an accumulation of work-hardening in the vicinity of a stress raiser. Head visualized the process of fatigue-crack propagation in the following manner: At the tip of an existing crack or flaw, the local strength would be exceeded in accordance with the Orowan mechanism. The crack would then advance an incremental amount into a region which had not yet been fully work-hardened. The region at the tip of the extended crack would then be hardened, and the process would be repeated over and over at an ever increasing rate since the stress-concentration factor at the crack tip would increase as the crack grew in length. The expression for the rate of fatigue-crack propagation developed from this model is of the following type:

$$\frac{dx}{dN} = 2\alpha x^{3/2} \quad (1)$$

From integration of equation (1) the crack length as a function of N is

$$x^{-\frac{1}{2}} = \alpha(C - N) \quad (2)$$

where α is a factor depending on stress, C is a constant, x is one-half the crack length, and N is the number of cycles. These equations are limited by a number of assumptions, among which are: that a linear law of work-hardening applies, that the mean stress is zero, and that the medium is of infinite extent. The number of arbitrary constants involved in the determination of the constant α precludes the general quantitative use of equations (1) and (2). Head compared the trend predicted by equation (2) with experimental results obtained for steel tested in rotating bending and, although the tests were not in keeping with all of his assumptions, found fairly good agreement over most of the range. Schijve did not find as good agreement from comparison of equation (2) with test results for axially loaded aluminum-alloy specimens at $R = 0$.

Weibull (ref. 3) has presented data on fatigue-crack propagation for a series of constant-load fatigue tests at $R = 0$ for sheet specimens of 2024-T3 and clad 7075-T6 aluminum alloys. He also developed semiempirical expressions for the rate of fatigue-crack propagation in these alloys. In deriving these expressions he assumed that the peak stress at the tip of the fatigue crack is the principal factor which determines the rate of fatigue-crack propagation.

The resultant expression was of the form

$$\frac{dx}{dN} = kS_{net}^n \quad (3)$$

where the constants k and n are to be determined empirically and depend upon the original specimen dimensions, the material, and possibly also the stress distribution. (Although Weibull was cognizant of the fact that the stress-concentration factor increased with crack length, no attempt was made to incorporate this fact into eq. (3).) Weibull checked the validity of equation (3) with test results and found good agreement except for very small cracks.

In a second investigation (ref. 4), Weibull found that for sheet specimens of aluminum alloys tested at constant amplitude of stress on the remaining net section at $R = 0$, the following expressions for the rate of fatigue-crack propagation gave good agreement with the data:

for 2024-T3,

$$\frac{\Delta x}{\Delta N} = 7.28 \times 10^{-7} (S_{net} - 1.4)^{1.75} \quad (4)$$

and for clad 7075-T6,

$$\frac{\Delta x}{\Delta N} = 2.94 \times 10^{-6} (S_{net})^{1.03} \quad (5)$$

Equation (4) indicates that for the particular 2024-T3 specimens tested, a stress exists below which a fatigue crack will not be propagated and that the rate of crack propagation depends solely on the net section stress and is independent of crack length. On the other hand, equation (5) indicates that no matter how low the stress level, the fatigue crack should be propagated.

Weibull's results (refs. 3 and 4) were obtained from specimens approximately 2 inches wide for maximum stresses between 5 and 20 ksi at

$R = 0$. He made the further observation (ref. 5) that the rate of fatigue-crack propagation is proportional to the width of the specimen. However, no data were presented to illustrate this effect.

This brief review indicates that considerably more quantitative information is required before the rate of fatigue-crack propagation in aluminum alloys can be predicted. Much more information is needed for the rate of fatigue-crack propagation at other values of R and for variable-amplitude loading. The review also reveals that the theoretical approach of Head is too qualitative because of the number of not readily determined constants involved, whereas the semiempirical approach of Weibull is too restrictive (i.e., to certain specimen shapes and test conditions) to be generally applicable. The method described herein will attempt to be more quantitative and more general than the previous approaches to the problem of the rate of fatigue-crack propagation.

Derivation of Equations

At the present time the complex nature of the process of fatigue-crack propagation precludes the derivation of expressions for the rate of propagation based solely on theoretical considerations. However, theoretical considerations can indicate which parameters are of importance, and useful results may be obtained through a semiempirical approach. Such an approach is adopted in the present paper.

In order to formulate an expression for the rate of fatigue-crack propagation, a physical concept of the process is required. For this purpose the process is considered to consist of two stages as in reference 2: during the first stage the material in a critical region at the tip of a crack is cyclically work-hardened up to the fracture strength of the material; during the second stage the crack is propagated an incremental amount into material which has not been work-hardened. Then the first stage is repeated, and so forth.

The extent of crack growth during the second stage will depend inversely upon the amount of plastic deformation required to advance the fracture front. Hence, it would be expected that in relatively brittle materials the extent of this advance would be greater than in more ductile materials.

In order to clarify the role of the work-hardening stage, some of the main points of Orowan's theory (ref. 6) are briefly reviewed. According to this theory, in any metal object there exist certain weak sites which will deform plastically while the remainder of the body remains elastic, provided the yield stress σ_y of the sites is exceeded. During cyclic loading the local stress at these sites increases because of the cumulative effects of work-hardening, and when the local stress

is raised to the local fracture strength, a fatigue crack is nucleated. (Unfortunately, the local fracture strength is a quantity which has not yet been quantitatively defined.)

Although the material at the critical sites may be thought of as hardening to the fracture strength, the work of Wood and Segall (ref. 7) has shown that there is a limit to the amount of overall hardening which can be developed through cyclic loading in a specimen for a given plastic-strain amplitude. In their experiments, this limiting value varies approximately as the square root of the plastic-strain amplitude. Once this limit has been reached, the specimen can be cycled indefinitely without a further change in the yield level of the material. The fact that the material yield strength leveled off instead of rising indefinitely was attributed to a process of stress relaxation.

In the present investigation, the first-stage process of work-hardening at the tip of the fatigue crack is considered to involve both the Orowan concept and the findings of Wood and Segall, with the addition that the stress-concentration factor for the crack K_N is taken into account. A method for the computation of stress-concentration factors for fatigue cracks has been presented in reference 8 and a brief review is given in the appendix of this paper. According to Wood and Segall, the total increase in yield strength developed through work-hardening is approximately proportional to the square root of the plastic-strain amplitude. In the present case the strain amplitude and hence the amount of hardening developed for the material at the tip of the crack is a function of the product of K_N , the stress-concentration factor, and S_{net} , the net section stress based on the instantaneous remaining area. Values of this product within the elastic range of the material correspond directly to the peak stress in a region at the tip of the fatigue crack. Beyond the elastic range, very high values even with respect to the static strength of the material may be obtained. However, because of plasticity and stress relaxation, the actual stresses will be much lower. For such cases no attempt is made to fix their exact magnitudes in this paper. Within this highly stressed region lie the damage nuclei of the Orowan type which are work-hardened up to the fracture strength, while the peak stress of the region as a whole may meanwhile have leveled off at some lesser value. In some cases it develops that, when $K_N S_{net}$ is in the elastic range, the fatigue cracks will still be propagated. This observation lends support to the idea that the critical sites which are being work-hardened are of even smaller dimensions than that of the region of peak stress. This interpretation is in contrast with Head's concept, which considers that the entire region at the tip of the crack makes up the critical site.

During the work-hardening stage for a given material the number of cycles required to raise the stress at the critical site up to the fracture strength of the material depends upon $K_N S_{net}$ and the endurance limit of the material. This latter value is assumed to be known from tests of unnotched specimens. Where the existence of an endurance limit is not clear, the stress at 10^8 cycles will be taken. For values of $K_N S_{net}$ below the endurance limit the work-hardening stage cannot lead to the formation of a crack, while for $K_N S_{net}$ values in excess of the endurance limit a crack will eventually be nucleated.

In order to formulate an expression for the rate of fatigue-crack propagation, let η be the number of cycles elapsed in a particular stage 1 upon which attention has been focused since the preceding stage 2, and let $d\sigma/d\eta$ be interpreted as the rate of increase of stress per cycle at a critical site during this first stage. Denote the total number of cycles involved from the start to the finish of this first stage by ΔN . Then the total number of cycles to propagate a crack over some large distance will be the sum of the various values of ΔN involved if no cycles are involved in the second stage. If it is assumed that the rate of increase of stress at the critical site is inversely proportional to the number of cycles η since the last increment of crack growth and that the rate for a propagating crack also depends upon $K_N S_{net}$ and the endurance limit, the rate of increase of stress can be expressed as

$$\frac{d\sigma}{d\eta} = \frac{1}{\eta} f(K_N S_{net}, S_e) \quad (6)$$

When this expression is integrated between the local yield strength σ_y and the local fracture strength σ_f , the following expressions are obtained

$$\log_e \Delta N = f_1(K_N S_{net}, S_e) \int_{\sigma_y}^{\sigma_f} \frac{d\sigma}{\sigma} \quad (7)$$

or

$$\log_e \Delta N = C_1 f_1(K_N S_{net}, S_e) \quad (8)$$

where

$$C_1 = \int_{\sigma_y}^{\sigma_f} d\sigma$$

Therefore,

$$\Delta N = e^{C_1 f_1(K_{NS_{net}}, S_e)} \quad (9)$$

The extent of incremental crack growth during the second stage also depends upon the value of $K_{NS_{net}}$ and may be expressed as

$$\Delta x = f_2(K_{NS_{net}}) \quad (10)$$

It is assumed that the time required for this incremental growth is small compared with the period of cycling. The average rate of fatigue-crack propagation may then be expressed as

$$r = \frac{\Delta x}{\Delta N} = \frac{f_2(K_{NS_{net}})}{e^{C_1 f_1(K_{NS_{net}}, S_e)}} \quad (11)$$

or

$$\log_{10} r = \log_{10} f_2(K_{NS_{net}}) - \frac{C_1}{2.3} f_1(K_{NS_{net}}, S_e) \quad (12)$$

Equation (12) is not of quantitative value, but shows that the rate of fatigue-crack propagation for a given material is a function solely of the parameter $K_{NS_{net}}$. The boundary condition is imposed that for $K_{NS_{net}}$ equal to or less than the endurance limit, the rate of fatigue-crack propagation should be zero. An expression for the rate of fatigue-crack propagation can be obtained only when some data are available, but once obtained can be extended to any other stress level or configuration for the material. A description of the specimens and tests of the present investigation used to obtain such an expression is given in the following section.

SPECIMENS AND TESTS

Specimen Preparation

Sheet material was chosen for this investigation because of its importance in aircraft structures and also because of the relative ease with which crack propagation can be studied in it. All specimens were made from single sheets of 2024-T3 and 7075-T6 aluminum alloys, nominally 0.102-inch thick. Blanks, 2 by $17\frac{1}{2}$ inches and 12 by 35 inches, were sheared from these sheets parallel to the rolling direction, and a number of standard tensile specimens were machined from various locations in the original sheets. Figure 1 gives the configurations of the crack-propagation test specimens. A $\frac{1}{16}$ -inch-diameter hole was drilled at the center of each blank and a $\frac{1}{32}$ -inch-deep notch was cut in each side of the hole with a nylon thread impregnated with a fine valve-grinding compound. The thread was drawn repeatedly with a reciprocating motion across the edge to be cut. The procedure resulted in remarkably consistent radii of 0.005 inch with an error of approximately ± 0.0003 inch. A 30-power microscope comparator was used to spot check the notch radii. These configurations had computed theoretical stress-concentration factors, K_T , of 7.4 and 7.9 for specimens 2 and 12 inches wide, respectively.

The surface area on one face of each specimen through which a crack was expected to travel was polished to a bright finish with No. 600 aluminum oxide powder to afford maximum contrast between the crack and the uncracked material. The 7075-T6 material exhibited a brighter final surface than did the 2024-T3. Fine longitudinal lines were inscribed with a razor blade to mark intervals in the path of the crack. No stress concentration due to these lines was expected since they were in the direction of loading. The distance from the center of the specimen to each line was measured before testing and the lines were numbered to facilitate identification during testing.

Equipment and Test Technique

Three types of testing machines were used in the investigation of fatigue-crack propagation:

(1) Subresonant-type fatigue machines were used for those specimens which were expected to survive for more than approximately 5,000 cycles. These machines operated at 1,800 cpm and had a capacity of $\pm 20,000$ pounds (ref. 9). The cycles counter read in hundreds of cycles.

(2) A 100,000-pound-capacity hydraulic fatigue machine operating at 1,200 cpm was used for tests requiring more than 5,000 cycles but which were beyond the capacity of the subresonant machines. The cycles counter read in hundreds of cycles.

(3) Those specimens which were expected to last less than 5,000 cycles were tested in a 120,000-pound-capacity hydraulic jack (ref. 10) in which the maximum speeds of cycling were about 50 and 20 cpm for specimens 2 and 12 inches wide, respectively. The cycles counter read directly in cycles.

In all tests, loads were continuously monitored by measuring the output of a bridge circuit whose active elements were wire-resistance strain gages. These gages were fixed to weighbars through which the load was transmitted to the specimen. Monitoring precision was approximately ± 1 percent.

The cracks were observed on only one face of the specimen through two 30-power microscopes and were illuminated by a stroboscopic light in the two faster machines to allow continuous observation of crack growth without interruption of the tests.

Tests were conducted in the range of S_0 up to 50 ksi. The initial minimum nominal stress was 1 ksi for all tests, and in general, two specimens were tested at each value of S_0 except as otherwise noted. The maximum and minimum loads were kept constant throughout each test.

The number of load cycles required to propagate the crack to each line was recorded until either complete failure occurred or the large loss of cross-sectional area made it impossible to control the loading accurately. At this stage the rate of fatigue-crack propagation was quite high and failure was imminent.

In order to determine the endurance limit of a specimen containing a fatigue crack, a number of tests were conducted on specimens 2 inches wide at values of S_0 which bracketed the endurance limit. After growing the cracks to a predetermined length at $S_0 = 10$ ksi, each of these specimens was tested at a particular stress level below 10 ksi in order to determine whether the crack would continue to be propagated at the lower level. The highest stress level S_0 which did not cause crack growth in 10^8 cycles was considered to be the endurance limit for a 2-inch-wide specimen containing fatigue cracks.

In addition, tensile tests were performed to determine the 0.2-percent-offset yield stress, the ultimate strength, the percent elongation, and the Young's modulus of the materials.

RESULTS AND DISCUSSION

The mechanical properties of the materials are given in table I. The crack-propagation test results are summarized in table II, which gives the number of cycles required to extend the crack from a length of 0.2 inch. This length was chosen for several reasons: It is quite difficult to determine precisely the number of cycles to crack initiation because of both the distortion in the region of the notch and the fact that the minimum size of crack which may be detected is a function of the magnification used. On the other hand, once a crack had formed and grown large enough to be detected, its progress was relatively easy to follow. Also, at a length of 0.2 inch it was felt that the rate of propagation no longer was affected by the original notch but depended only upon conditions in the immediate vicinity of the tip of the crack.

The crack lengths given are the averages from two specimens at each stress level of 10 ksi or greater. Only one specimen was tested at each value of S_0 below 10 ksi. The final 5 percent of crack life was omitted in each test since it was felt that loading inaccuracies during that period were excessive. The cracks grew symmetrically, with eccentricities seldom exceeding 0.1 inch. The fatigue cracks initially grew in planes perpendicular to the sheet but after a distance which was inversely proportional to a power of S_0 the cracks grew at 45° to the thickness direction. Within experimental accuracy, however, this change did not have a significant effect on the rate of fatigue-crack propagation.

Table II also includes the total number of cycles to failure. The S_0 -N curves for complete failure are shown in figures 2, 3, 4, and 5.

The crack propagation rates were determined as follows: Each crack length was plotted against the number of cycles required to obtain each length. Average curves were then computed for each stress level and are shown in figure 6 as solid lines. The dashed lines in this figure are discussed subsequently in this paper. The rate of crack propagation (slope) was found graphically from these average curves. All crack propagation rates presented in this paper refer to the progress of only one end of the crack relative to the center line of the specimen.

The scatter in life was quite small for both crack life and total life to failure. The effects of cycling frequency are of minor importance and not readily predictable, for as can be seen in figure 6 for $S_0 = 30$ ksi, the 2024-T3 aluminum alloy exhibits a slightly higher average propagation rate at 50 cpm than at 1,800 cpm; whereas the 7075-T6 aluminum alloy, the reverse is true. For identical test conditions the crack propagation rate for 7075-T6 was always greater than that for 2024-T3.

As shown in table II endurance limits (or the stress at 10^8 cycles) were found for both 2024-T3 and 7075-T6 materials containing fatigue

cracks. This contrasts with Weibull's suggested formula for crack propagation rate (eq. (5)), which implies that no endurance limit exists for 7075-T6 material containing fatigue cracks.

COMPARISON WITH THEORIES

Present Theory - Present Test Results

In order to compare the results of the tests with the predictions of the theory, it is necessary to know the Neuber material constants for these aluminum alloys (2024-T3 and 7075-T6). (See appendix.) These constants have been previously evaluated in reference 8 through analysis of tensile tests run to failure of parts containing stress raisers of known radii. However, the present data afford an opportunity to reevaluate these constants in a more sensitive fashion, since no correction for plasticity effects is required.

As mentioned previously, whether a fatigue crack will be propagated is governed by the relation of the value of $K_N S_{net}$ to the endurance limit of the material. In reference 8 it was found that the Neuber material constant ρ' and the effective radius of a fatigue crack ρ_e were of the same order, and as a simplification the two were assumed to be equal. The same assumption is made in the present case, and appendix equation (A3) becomes

$$K_N = 1 + \frac{1}{2}(K_H - 1) \sqrt{\frac{x}{\rho_e}} \quad (13)$$

where x is one-half the length of the crack and K_H is the stress-concentration factor for a hole of radius x .

From reference 9, the endurance limit (or the stress at 10^8 cycles) for unnotched sheet specimens of 2024-T3 and 7075-T6 for values of R appropriate to the present tests was obtained and is 34 ksi for both materials. From the data of the present investigation, stresses and corresponding crack lengths for which cracks are not propagated are known. Consequently, through the relation

$$K_N S_{net} = S_e \quad (14)$$

the only unknown ρ_e appearing in equation (13) can be evaluated. The results of such calculations for ρ_e are given in table III, together with the results from reference 8 for static tests. Because of uncertainties due to scatter in the determination of the endurance limits for unnotched specimens, the present values of ρ_e are given to one significant figure only. It is seen that the two dissimilar types of

tests give results for the constants which are in good agreement. The values of ρ_e determined through use of equation (14) will be adopted in this report; these values are 0.003 and 0.002 inch for 2024-T3 and 7075-T6, respectively.

Once the values of ρ_e have been established, K_N (eq. (13)) can be evaluated for various crack lengths. In figure 7 a plot of K_N against crack length covering the range of the present tests is presented for each material and specimen width. With K_N known, the product $K_N S_{net}$ can be obtained at any stage during the propagation of a fatigue crack.

In figures 8 to 11, plots of $K_N S_{net}$ against the rate of fatigue-crack propagation are presented. The data for different widths and different materials have been plotted separately for clarity. In each figure the rate is essentially a single-valued function of the parameter $K_N S_{net}$.

From equation (12), the rate is seen to depend upon $K_N S_{net}$ and the endurance limit S_e . An equation which fits the test data and incorporates these quantities in addition to satisfying the boundary condition that the rate should go to zero as $K_N S_{net}$ approaches the endurance limit is

$$\log_{10} r = 0.00509 K_N S_{net} - 5.472 - \frac{34}{K_N S_{net} - 34} \quad (15)$$

This equation has been plotted as the dashed line in figures 8 to 11 and is seen to agree well with all the data, irrespective of material or specimen width. Although agreement for a particular material irrespective of width was anticipated, it was not expected that a single curve would fit the data for both materials.

The principal discrepancy between the data and the general curve occurs for 2024-T3 specimens tested at an initial maximum net section stress of 50 ksi. A possible explanation of this discrepancy is that the net section stress for the material is above the elastic limit, and therefore a modification of the work-hardening process and, consequently, of the rate of fatigue-crack propagation might be expected.

Although the parameter $K_N S_{net}$ in these tests takes on values up to 600 ksi, the work of Wood and Segall (ref. 7) tends to show that the actual stress in the region at the tip of the crack would never attain such a high value but would level off at some lower value. Just what values are developed is not known, but the present results indicate that

the level attained is a function of $K_N S_{net}$ in the small constrained region at the tip of the crack.

Since the number of cycles to develop a crack of a certain length may be of practical interest, it is desirable that the rate equation (15) be integrated. As it is not possible to perform this integration directly, a numerical integration must be employed. For the sake of comparison, equation (15) has been integrated for one stress level (30 ksi) for both materials in the two widths and the results are compared with the experimental results in figure 6 (short-dashed lines). In view of the fact that small deviations in the rate in the early stages can lead to large deviations in N after integration and also that the plots are on a linear N rather than a $\log N$ basis, the agreement found is considered to be reasonably satisfactory.

The large range of experimental data obtained in this investigation provides an opportunity to evaluate and compare the present theory with other studies of fatigue-crack propagation, and this is done in the following sections.

Present Theory - Weibull's Results

Data from Weibull's constant-load tests (ref. 3) are shown in figure 12. In these tests K_N and S_{net} increase with crack length. Agreement with the general curve is seen to be fairly good and lends support to the $K_N S_{net}$ approach. Clad 7075-T6 exhibits a higher rate of fatigue-crack propagation than the bare 7075-T6 material tested in the present investigation, and such an effect is not unexpected. It is interesting to note that coating the clad material with kerosene brings the results into better agreement with the general curve.

A more critical evaluation is obtained through an examination of Weibull's data for constant-stress tests (ref. 4) plotted in figure 13. In these tests the load was repeatedly adjusted after short intervals to maintain a constant stress. Each point in figure 13 represents the average rate during this interval and each type of symbol represents the data from one specimen. According to Weibull the data should lie on a series of horizontal lines, since S_{net} is constant for any stress level. The present theory holds that although S_{net} is constant, K_N increases as the crack length increases, and consequently these data should lie along the general curve. The fact that the data do indeed generally follow the curve rather than fall along horizontal lines further substantiates the present theory.

It should also be pointed out that for small cracks Weibull did not get good agreement between his theory and his data, whereas in the present case when his data are plotted in terms of $K_N S_{net}$, even the small-crack data fall along the generalized curve.

Weibull's Theory - Present Results

The present data have been plotted in terms of S_{net} in figure 14. In this figure the rate data for both widths are presented in terms of the rate of fatigue-crack propagation as a percentage of specimen width in order to check Weibull's rate-width relations.

According to Weibull, crack propagation depends solely on S_{net} , and the data for a particular width of the specimens tested should lie along a single curve which is a unique function of S_{net} . Examination of the figure shows that this is approximately true for the 2-inch-wide specimens but is not true for the 12-inch-wide specimens. It is considered that the better agreement found for the 2-inch-wide specimens is essentially due to a smaller variation of K_N with crack length for these specimens than for the 12-inch-wide specimens.

Weibull also stated that the rate of fatigue-crack propagation is proportional to the width of the specimen. If this were the case, the data for both widths when plotted in terms of percentage of width per cycle against S_{net} should lie along the same curve. Although figure 14 shows a degree of overlap of the curves, the overall agreement is not considered to be satisfactory.

Head's Theory - Present Results

The only quantitative conclusion of Head's which can be compared with the present results is that the data plotted in terms of $x^{-\frac{1}{2}}$ against N should fall along straight lines. Since the type of test utilized herein is not in accord with several of Head's assumptions, good agreement would be rather surprising. Nevertheless, the data do fall on approximately straight lines as seen in figure 15. Since this is the case, a possibility for a simple method for integration of the rate equation (15) presents itself.

The several unknown constants in Head's theory can be combined into a single stress-dependent constant which determines the slopes of the

straight lines in figure 15. This constant α , which appears in the rate expression developed by Head (eq. (1)), is

$$\frac{dx}{dN} = 2\alpha x^{3/2}$$

In the present derivation the rate is given by the more complex expression

$$\frac{dx}{dN} = \log_{10}^{-1} \left(0.00509 K_N S_{net} - 5.472 - \frac{34}{K_N S_{net} - 34} \right) \quad (16)$$

Since both expressions appear to give reasonably good results for the rate of fatigue-crack propagation, the right-hand sides of each can be equated and solved for the unknown α :

$$\alpha = \frac{1}{2} x^{-3/2} \log_{10}^{-1} \left(0.00509 K_N S_{net} - 5.472 - \frac{34}{K_N S_{net} - 34} \right) \quad (17)$$

Since α is supposed to be a constant for a given stress level, it follows that the product on the right-hand side must also be a constant for that stress level. In order to check on this conclusion, α has been evaluated for the present data and the results are given in table IV. The results indicate that α is approximately constant, at least for short cracks although a general increase with crack length is noted. The variation of α with crack length is seen to be much less than the variation of α with the stress level S_0 . The fact that α is approximately constant for a given stress level S_0 and specimen width leads to a simpler method for obtaining quantitative predictions. An average value of α for a specimen and stress level can be computed. Since most of the life is spent in the short-crack region, values of α in this region should be more heavily weighted in obtaining the average. This can be done by multiplying α by the reciprocal of the rate as determined by equation (15) and determining the thus weighted average. These averages are also given in table IV. (In many instances, especially for a short crack length, sufficiently accurate results may be obtained by a single determination of α .)

These values for α may then be used to evaluate the number of cycles required to produce a crack of a given length in equation (2) expressed as:

$$N = C - \frac{1}{\alpha} x^{-\frac{1}{2}}$$

where N is the number of cycles measured from an initial crack length and C is a constant of integration (which may be determined from the crack length when N is zero).

In figure 6 computed curves based on this expression for N are compared with experimental curves plotted from the data of table II. In general, the agreement is seen to be good. The maximum discrepancy is of the order of 2:1 except when S_{net} exceeds the yield point and except for very low stresses. Accurate predictions of crack propagation rates for low values of $K_N S_{net}$ are difficult because of the very steep slope in that region of the curve of rate against $K_N S_{net}$. Whether good agreement would be found for other types of specimens and other loading conditions remains to be seen.

CONCLUDING REMARKS

A general method has been developed for the determination of fatigue-crack propagation rates. An extensive series of tests has been conducted on sheet specimens of 2024-T3 and 7075-T6 aluminum alloys in order to provide a check on the theoretical predictions and to evaluate certain empirical constants. The dependence of the rate of fatigue-crack propagation on the parameter $K_N S_{net}$ (theoretical stress-concentration factor modified for size effect times net section stress) has been demonstrated, and a general means is thereby provided for the determination of fatigue-crack propagation rates.

Incidental to the main purpose of the paper, it is of interest to note that endurance limits (or the stress at 10^8 cycles) of specimens containing fatigue cracks have been established, and that these endurance limits can be utilized in the determination of the effective radius of curvature of a fatigue crack. The fact that the rate of fatigue crack propagation for both 2024-T3 and 7075-T6 can be given by the same expression is also noteworthy. As has been reported in the literature, crack growth in 7075-T6 is more rapid than in 2024-T3 tested under similar conditions. This fact is reflected in the smaller value of ρ_e (effective radius of fatigue crack) for 7075-T6; namely, 0.002 inch, as compared with the value for 2024-T3 of 0.003 inch.

Through a combination of the present theory and the theory of Head, an approximation has been made which enables the rate expression to be

easily integrated in order to obtain crack lengths as a function of the number of load cycles.

In conclusion, it should be pointed out that the present investigation has been concerned only with simple specimens tested at an R value of approximately zero, where R is the ratio of minimum stress to maximum stress. Information is needed on other R values of interest and also on the effect of variable-amplitude loading on fatigue-crack propagation, so that in combination with aircraft-load statistics a rational fail-safe program of periodic inspection might be set up.

Langley Aeronautical Laboratory,
National Advisory Committee for Aeronautics,
Langley Field, Va., July 14, 1958.

APPENDIX

CALCULATION OF K_N

The method of calculation of K_N , the stress-concentration factor corrected for size effect, is presented in this appendix. This method was developed in reference 8, and is given in greater detail therein.

For the case of a sheet containing a central, symmetrical crack, such as in the present investigation, the stress-concentration factor for a circular hole K_H of diameter equal to the total length of the crack is determined from Howland's curve (ref. 11) shown in figure 16. The crack is then considered to be an ellipse of major axis equal to the total length of the crack, and the stress-concentration factor for such a configuration is assumed to be related to that for a hole as follows:

$$K_E = 1 + (K_H - 1) \sqrt{\frac{a}{\rho}} \quad (A1)$$

where K_E is the stress concentration factor for the ellipse of semi-major axis a and of tip radius ρ .

In order to obtain an expression for the stress-concentration factor for a crack, the effect radius ρ_e is substituted for ρ , and the crack length is substituted for the major axis of the ellipse.

The final step in computing the stress-concentration factor is to make a correction for size effect. Such a correction has been made by Neuber in the following manner:

$$K_N = 1 + \frac{K_E - 1}{1 + \sqrt{\frac{\rho'}{\rho_e}}} \quad (A2)$$

where ρ' is a material constant which is determined empirically.

Substituting, there is obtained

$$K_N = 1 + \frac{(K_H - 1) \sqrt{\frac{a}{\rho_e}}}{1 + \sqrt{\frac{\rho'}{\rho_e}}} \quad (A3)$$

REFERENCES

1. Schijve, J.: Fatigue Crack Propagation in Light Alloys. NLL-TN M.2010, Nationaal Luchtvaartlaboratorium (Amsterdam), July 1956.
2. Head, A. K.: The Growth of Fatigue Cracks. Phil. Mag., ser. 7, vol. 44, no. 356, Sept. 1953, pp. 925-938.
3. Weibull, Waloddi: The Propagation of Fatigue Cracks in Light-Alloy Plates. SAAB TN 25, Saab Aircraft Co. (Linköping, Sweden), Jan. 12, 1954.
4. Weibull, Waloddi: Effect of Crack Length and Stress Amplitude on Growth of Fatigue Cracks. Rep. 65, Aero. Res. Inst. of Sweden (Stockholm), 1956.
5. Weibull, W.: Discussion of "Fatigue Cracks as Stress Raisers and Their Response to Cyclic Loading" by C. E. Phillips. Fatigue in Aircraft Structures, Alfred M. Freudenthal, ed., Academic Press, Inc. (New York), 1956, pp. 119-121.
6. Orowan, E.: Theory of the Fatigue of Metals. Proc. Roy. Soc. (London), ser. A, vol. 171, no. 944, May 1, 1939, pp. 79-106.
7. Wood, W. A., and Segall, R. L.: Annealed Metals Under Alternating Plastic Strain. Proc. Roy. Soc. (London), ser. A, vol. 242, no. 1229, Oct. 29, 1957, pp. 180-188.
8. McEvily, Arthur J., Jr., Illg, Walter, and Hardrath, Herbert F.: Static Strength of Aluminum-Alloy Specimens Containing Fatigue Cracks. NACA TN 3816, 1956.
9. Grover, H. J., Hyler, W. S., Kuhn, Paul, Landers, Charles B., and Howell, F. M.: Axial-Load Fatigue Properties of 24S-T and 75S-T Aluminum Alloy as Determined in Several Laboratories. NACA Rep. 1190, 1954. (Supersedes NACA TN 2928.)
10. Illg, Walter: Fatigue Tests on Notched and Unnotched Sheet Specimens of 2024-T3 and 7075-T6 Aluminum Alloys and of SAE 4130 Steel With Special Consideration of the Life Range From 2 to 10,000 Cycles. NACA TN 3866, 1956.
11. Howland, R. C. J.: On the Stresses in the Neighbourhood of a Circular Hole in a Strip Under Tension. Phil. Trans. Roy. Soc. (London), ser. A, vol. 229, no. 671, Jan. 6, 1930, pp. 49-86.

TABLE I.- AVERAGE MECHANICAL PROPERTIES OF ALUMINUM ALLOYS TESTED

	2024-T3	7075-T6
Yield stress (0.2-percent offset), ksi . . .	51.2	77.9
Ultimate strength, ksi	71.3	82.9
Total elongation (based on 2-inch gage length), percent	22.3	11.8
Young's modulus, ksi	10.61×10^3	10.60×10^3
Number of specimens	7	9

TABLE II.- AVERAGE NUMBER OF CYCLES REQUIRED TO EXTEND FATIGUE CRACKS FROM 0.2 INCH, AND TOTAL LIFE TO FAILURE

(a) 2-inch-wide specimens

Stress level, S_0 , ksi	Cycling frequency, cps	Number of tests	Initial crack length, in.	Number of cycles to extend crack from 0.2 in. to a length of -								Total life, cycles
				0.25 in.	0.30 in.	0.40 in.	0.50 in.	0.60 in.	0.70 in.	0.80 in.	1.00 in.	
2024-T3 aluminum alloy												
^a 4.0	1,800	1	0.50	Crack did not propagate in 10^8 cycles								-----
^a 5.1	1,800	1	.16	Crack did not propagate in 10^8 cycles								-----
^a 5.3	1,800	1	.50	Failed								-----
^a 6.0	1,800	1	.13	Crack did not propagate in 10^8 cycles								-----
^a 6.5	1,800	1	.13	Crack did not propagate in 10^8 cycles								-----
^a 7.1	1,800	1	.14	217,500	392,500	640,000	841,500	947,500	991,000	1,013,000	-----	
10	1,800	2	---	94,500	164,000	235,000	266,000	284,500	297,500	308,500	588,000 736,000	
14.5	1,800	2	---	11,700	19,800	32,500	40,600	46,200	50,800	55,400	62,400	104,000 116,000
20	1,800	2	---	4,000	7,200	12,400	16,300	19,400	21,700	23,800	26,300	45,600 43,200
25	1,800	2	---	2,400	4,200	7,000	9,300	10,900	12,000	12,600	-----	22,500 22,300
30	1,800	2	---	1,600	3,000	4,800	6,300	7,100	-----	-----	-----	13,600 14,500
30	50	1	---	1,070	1,890	3,015	3,800	4,350	-----	-----	-----	8,900
40	50	2	---	540	920	1,346	1,538	-----	-----	-----	-----	2,310 3,600
50	50	2	---	172	220	238	-----	-----	-----	-----	-----	1,200 820
7075-T6 aluminum alloy												
^a 5.2	1,800	1	0.91	Crack did not propagate in 10^8 cycles								-----
^a 5.5	1,800	1	.50	Crack did not propagate in 10^8 cycles								-----
^a 4.7	1,800	1	.50	Failed								-----
^a 5.1	1,800	1	.16	Crack did not propagate in 10^8 cycles								-----
^a 5.5	1,800	1	.17	Crack did not propagate in 10^8 cycles								-----
^a 5.6	1,800	1	.16	180,000	335,000	577,500	775,000	900,000	982,500	1,020,000	-----	
^a 6.6	1,800	1	.16	160,000	297,000	488,000	587,000	620,000	641,000	-----	-----	
^a 7.1	1,800	1	.14	73,500	137,500	230,000	264,800	285,800	299,500	307,800	-----	
^a 7.6	1,800	1	.14	120,500	198,800	300,000	347,500	374,500	-----	-----	-----	
10	1,800	2	---	29,300	45,500	63,000	74,200	82,000	88,500	93,500	101,500	305,000 241,000
14.5	1,800	2	---	3,900	6,800	11,000	14,300	17,100	19,400	21,400	24,000	41,300 43,800
20	1,800	2	---	2,000	3,800	6,600	8,500	9,800	10,800	11,500	-----	20,400 21,700
25	1,800	2	---	1,300	2,500	4,100	5,100	5,800	-----	-----	-----	11,800 11,000
30	1,800	2	---	870	1,480	2,310	2,850	-----	-----	-----	-----	5,700 5,600
30	50	1	---	1,890	2,475	3,250	3,650	3,920	-----	-----	-----	6,040
40	40	2	---	374	635	930	1,075	-----	-----	-----	-----	2,960 2,280
50	50	2	---	142	210	274	314	-----	-----	-----	-----	989 825

^aCracks were initiated at 10 ksi.

TABLE II.- AVERAGE NUMBER OF CYCLES REQUIRED TO EXCEED FATIGUE CRACKS FROM 0.2 INCH, AND TOTAL LIFE TO FAILURE - Concluded

(b) 12-inch-wide specimens

Stress Level, S_0 , ksi	Cycling frequency, cps	Number of tests	Initial crack length, in.	Number of cycles to extend crack from 0.2 in. to a length of -									Total life, cycles
				0.30 in.	0.40 in.	0.50 in.	0.60 in.	0.80 in.	1.00 in.	1.40 in.	1.80 in.	2.40 in.	
2024-T3 aluminum alloy													
$S_{5.1}$	1,800	1	0.16	Crack did not propagate in 10^8 cycles									
10	1,800	2	---	70,000	98,000	109,000	132,000	155,000	170,000	194,000	210,000	230,000	472,000 494,000
14.5	1,800	2	---	13,400	22,400	28,900	34,400	41,600	50,300	60,900	66,100	74,500	117,000 117,000
20	1,200	2	---	5,900	10,500	14,400	17,800	23,600	27,600	32,100	34,200	35,500	50,300 51,000
25	1,200	2	---	2,800	5,200	7,600	9,800	13,000	14,400	16,000	16,400	16,900	27,300 21,700
30	1,200	2	---	1,800	3,100	4,100	4,700	5,500	5,900	6,400	-----	-----	10,900 9,400
40	20	2	---	513	890	1,068	1,185	1,345	1,430	1,490	-----	-----	2,300 2,420
50	20	2	---	95	130	142	157	164	-----	-----	-----	-----	2,070 2,970
7075-T6 aluminum alloy													
$S_{5.1}$	1,800	1	0.15	Crack did not propagate in 10^8 cycles									
10	1,800	2	---	24,900	40,100	50,600	58,500	70,600	79,800	95,300	105,000	109,500	205,000 258,000
14.5	1,800	2	---	6,000	10,500	14,000	17,000	21,600	24,800	29,200	31,500	33,000	56,600 45,700
20	1,200	2	---	3,400	5,900	7,400	8,700	10,700	11,800	12,900	-----	-----	23,400 18,000
25	1,200	2	---	2,000	3,300	4,300	4,900	5,600	6,000	6,400	-----	-----	9,900 9,500
30	1,200	2	---	940	1,580	1,910	2,120	2,410	-----	-----	-----	-----	4,600 4,400
40	20	2	---	335	499	588	645	715	-----	-----	-----	-----	1,640 1,670
50	20	2	---	113	159	186	203	-----	-----	-----	-----	-----	505 712

*Cracks were initiated at 10 ksi.

TABLE III.- COMPARISON OF VALUES OF ρ_e OBTAINED
FROM STATIC AND FATIGUE TESTS

Aluminum alloy	Values of ρ_e , in., from -		
	Static tests (ref. 8), 12-inch-wide specimens		Endurance tests, 2-inch-wide specimens
	60° V-notch	U-notch	Fatigue crack
2024-T3	0.0038	0.0057	0.003
7075-T6	.0019	.0028	.002

TABLE IV-- THE CONSTANT α USED IN INTERPOLATION OF RATE EXPRESSION, EQUATION (1)

(a) 2024-25, 2-inch-wide specimens

Crack length, in.	Values of α for stress level, S_0 , of -							
	7.1 ksi	10.0 ksi	14.5 ksi	20.0 ksi	25.0 ksi	30.0 ksi	40.0 ksi	50.0 ksi
0.29	0.0607×10^{-5}	0.9960×10^{-5}	3.628×10^{-5}	8.514×10^{-5}	15.40×10^{-5}	26.27×10^{-5}	69.75×10^{-5}	173.9×10^{-5}
.35	.0888	1.059	3.449	7.991	14.34	25.27	71.72	189.9
.41	.1724	1.126	3.367	7.489	13.74	23.32	76.51	218.2
.47	.2571	1.098	3.161	8.999	18.22	34.24	118.5	381.9
.53	.2749	1.118	3.226	7.515	15.21	28.97	98.97	318.9
.59	.3121	1.135	3.152	7.491	15.45	30.27	109.2	380.8
.65	.3778	1.228	3.265	8.014	17.00	34.54	136.5	499.2
.71	.4255	1.206	3.310	8.511	17.97	38.06	158.4	626.5
.77	.4395	1.277	3.411	8.790	19.88	45.00	194.6	1036
.83	.4865	1.365	3.610	10.10	23.01	52.94	256.5	-----
.89	.5359	1.432	3.737	11.20	27.46	64.06	342.0	-----
.95	.5805	1.527	4.215	13.06	33.60	82.47	481.1	-----
1.01	.6248	1.698	4.750	15.32	41.79	104.5	-----	-----
Weighted average	0.1420×10^{-5}	1.138×10^{-5}	3.443×10^{-5}	8.338×10^{-5}	16.32×10^{-5}	30.61×10^{-5}	94.27×10^{-5}	249.2×10^{-5}

(b) 7075-16, 2-inch-wide specimens

Crack length, in.	Values of α for stress level, S_0 , of -										
	5.6 ksi	6.6 ksi	7.0 ksi	7.6 ksi	10.0 ksi	14.5 ksi	20.0 ksi	25.0 ksi	30.0 ksi	40.0 ksi	50.0 ksi
0.29	0.0120×10^{-5}	0.0137×10^{-5}	0.2050×10^{-5}	0.4711×10^{-5}	1.612×10^{-5}	5.660×10^{-5}	12.68×10^{-5}	24.00×10^{-5}	42.60×10^{-5}	129.5×10^{-5}	366.8×10^{-5}
.35	.0506	.0290	.4372	.6762	1.947	5.368	12.98	25.27	47.13	157.1	505.5
.41	.0324	.0529	.5065	.6845	1.870	5.146	12.59	25.05	47.95	169.7	525.7
.47	.1598	.5819	.5665	.7244	2.065	5.136	12.29	26.12	52.24	197.6	724.4
.53	.2016	.4582	.6232	.7698	1.906	5.022	12.65	27.49	56.82	241.9	898.1
.59	.2216	.5150	.6710	.8585	1.966	5.119	13.42	30.27	65.54	299.6	1295.2
.65	.2671	.5397	.7285	.8500	1.889	5.181	14.05	33.19	74.20	364.5	-----
.71	.3002	.5752	.7529	.9102	1.962	5.319	15.13	35.81	86.29	461.0	-----
.77	.3600	.6174	.8058	.9513	2.050	5.691	17.16	38.86	107.8	617.4	-----
.83	.3928	.6627	.8604	1.029	2.188	6.175	19.27	51.44	134.7	-----	-----
.89	.4464	.7244	.8929	1.078	2.274	6.991	22.74	65.17	170.1	-----	-----
.95	.4811	.7941	.9774	1.161	2.474	7.788	27.49	81.70	256.7	-----	-----
1.01	.5505	.8498	1.045	1.296	2.689	8.916	34.13	107.5	450.6	-----	-----
Weighted average	0.0455×10^{-5}	0.3016×10^{-5}	0.4967×10^{-5}	0.7041×10^{-5}	1.967×10^{-5}	5.521×10^{-5}	13.99×10^{-5}	29.25×10^{-5}	58.79×10^{-5}	189.6×10^{-5}	540×10^{-5}

TABLE IV.- THE CONSTANT α USED IN INTEGRATION OF RATE EXPRESSION, EQUATION (1) - Concluded

(c) 2024-T3, 12-inch-wide specimens

Crack length, in.	Values of α for stress level, S_0 , of -						
	10.0 ksi	14.5 ksi	20.0 ksi	25.0 ksi	30.0 ksi	40.0 ksi	50.0 ksi
0.31	1.270×10^{-5}	4.221×10^{-5}	9.672×10^{-5}	18.11×10^{-5}	31.07×10^{-5}	87.70×10^{-5}	237.7×10^{-5}
.37	1.288	3.833	8.923	17.03	31.42	94.88	270.2
.43	1.279	3.661	8.526	16.30	31.09	100.3	305.9
.49	1.257	3.504	8.450	16.49	30.92	103.5	346.2
.55	1.266	3.363	8.114	16.47	31.90	112.7	395.3
.61	1.194	3.266	8.017	16.33	33.55	126.2	439.4
.67	1.160	3.120	7.736	16.30	33.78	131.5	495.1
.73	1.179	2.971	7.596	16.53	34.01	142.9	544.2
.79	1.128	2.880	7.533	16.52	35.25	153.1	614.3
.85	1.137	2.887	7.669	17.14	36.99	166.0	667.6
.91	1.108	2.851	7.737	17.43	38.28	177.6	-----
.97	1.081	2.813	7.698	18.36	40.71	198.4	-----
1.10	1.017	2.758	7.845	18.56	45.35	230.5	-----
1.30	.9636	2.624	8.014	19.65	50.57	299.6	-----
1.50	.9238	2.617	8.468	22.63	59.27	-----	-----
1.70	.8931	2.713	9.059	25.20	68.26	-----	-----
1.90	.8586	2.700	9.342	27.54	79.38	-----	-----
2.10	.8365	2.742	10.22	31.14	97.59	-----	-----
2.30	.8312	2.761	10.74	35.07	111.5	-----	-----
Weighted average	1.185×10^{-5}	3.361×10^{-5}	8.433×10^{-5}	17.44×10^{-5}	34.36×10^{-5}	113.6×10^{-5}	339.7×10^{-5}

(d) 7075-T6, 12-inch-wide specimens

Crack length, in.	Values of α for stress level, S_0 , of -						
	10.0 ksi	14.5 ksi	20.0 ksi	25.0 ksi	30.0 ksi	40.0 ksi	50.0 ksi
0.31	2.418×10^{-5}	6.721×10^{-5}	15.82×10^{-5}	29.51×10^{-5}	58.20×10^{-5}	196.7×10^{-5}	622.9×10^{-5}
.37	2.042	6.346	15.08	30.47	60.95	216.8	772.9
.43	2.608	6.018	14.79	31.59	63.19	245.7	907.7
.49	2.143	5.771	15.05	31.74	66.78	280.3	1072
.55	2.046	5.548	14.56	32.59	71.43	308.6	1266
.61	1.960	5.344	14.25	32.54	72.74	338.5	-----
.67	1.934	5.157	14.44	33.27	77.36	373.7	-----
.73	1.905	5.011	14.63	34.47	83.90	415.0	-----
.79	1.873	5.055	14.50	36.25	87.61	473.3	-----
.85	1.804	5.052	14.98	37.89	95.63	544.3	-----
.91	1.776	5.131	15.31	39.91	102.6	619.0	-----
.97	1.732	5.107	15.69	42.19	111.0	-----	-----
1.10	1.692	5.210	16.67	34.94	127.5	-----	-----
1.30	1.574	5.037	17.84	34.38	162.2	-----	-----
1.50	1.540	5.119	19.63	63.89	234.8	-----	-----
1.70	1.499	5.295	21.37	73.36	242.4	-----	-----
1.90	1.485	5.400	23.49	83.70	-----	-----	-----
2.10	1.464	5.669	26.02	100.4	-----	-----	-----
2.30	1.379	5.879	28.79	117.6	-----	-----	-----
Weighted average	2.003×10^{-5}	5.942×10^{-5}	15.41×10^{-5}	34.20×10^{-5}	69.16×10^{-5}	267.2×10^{-5}	811.0×10^{-5}

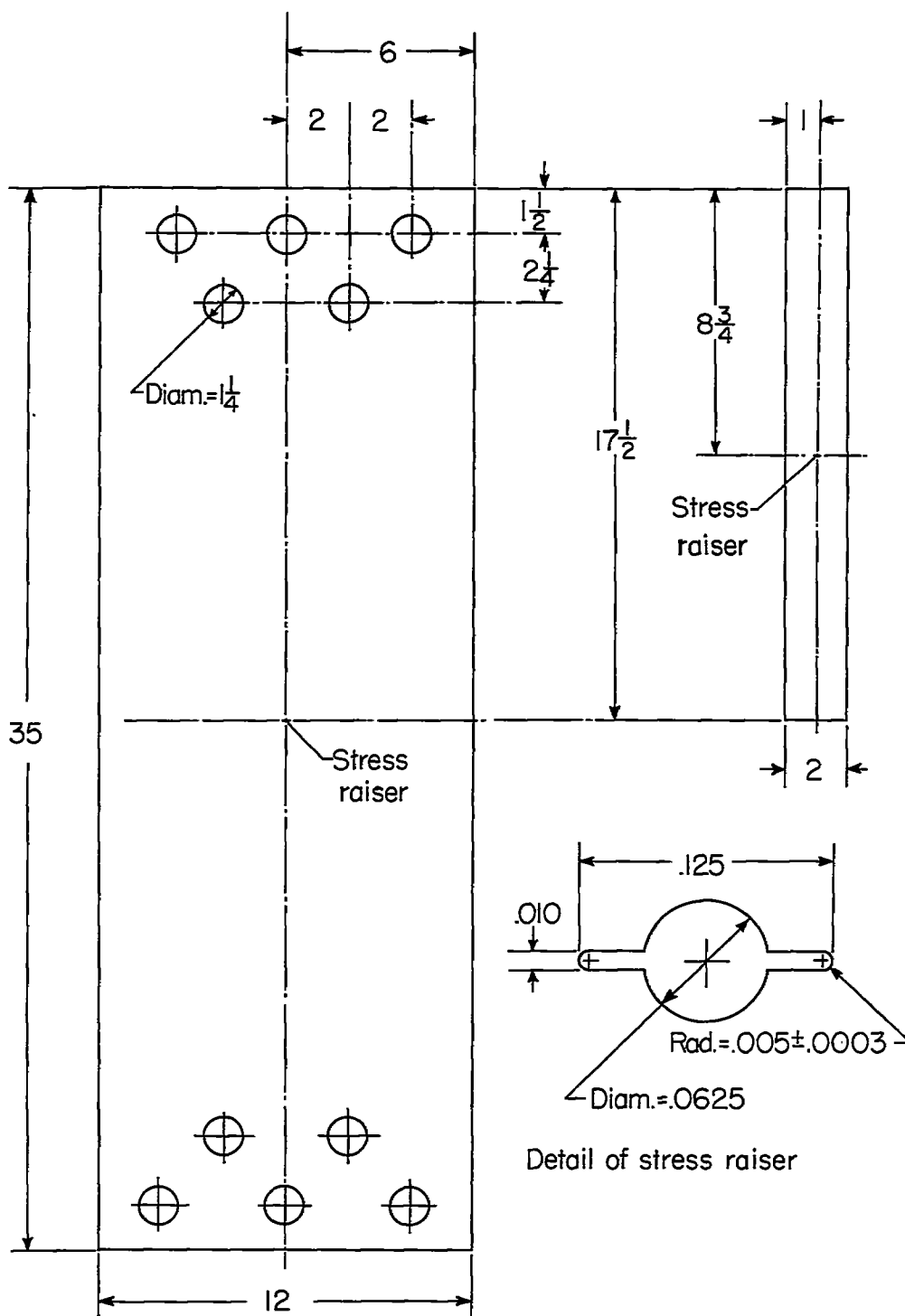


Figure 1.- Configurations of crack-propagation specimens.

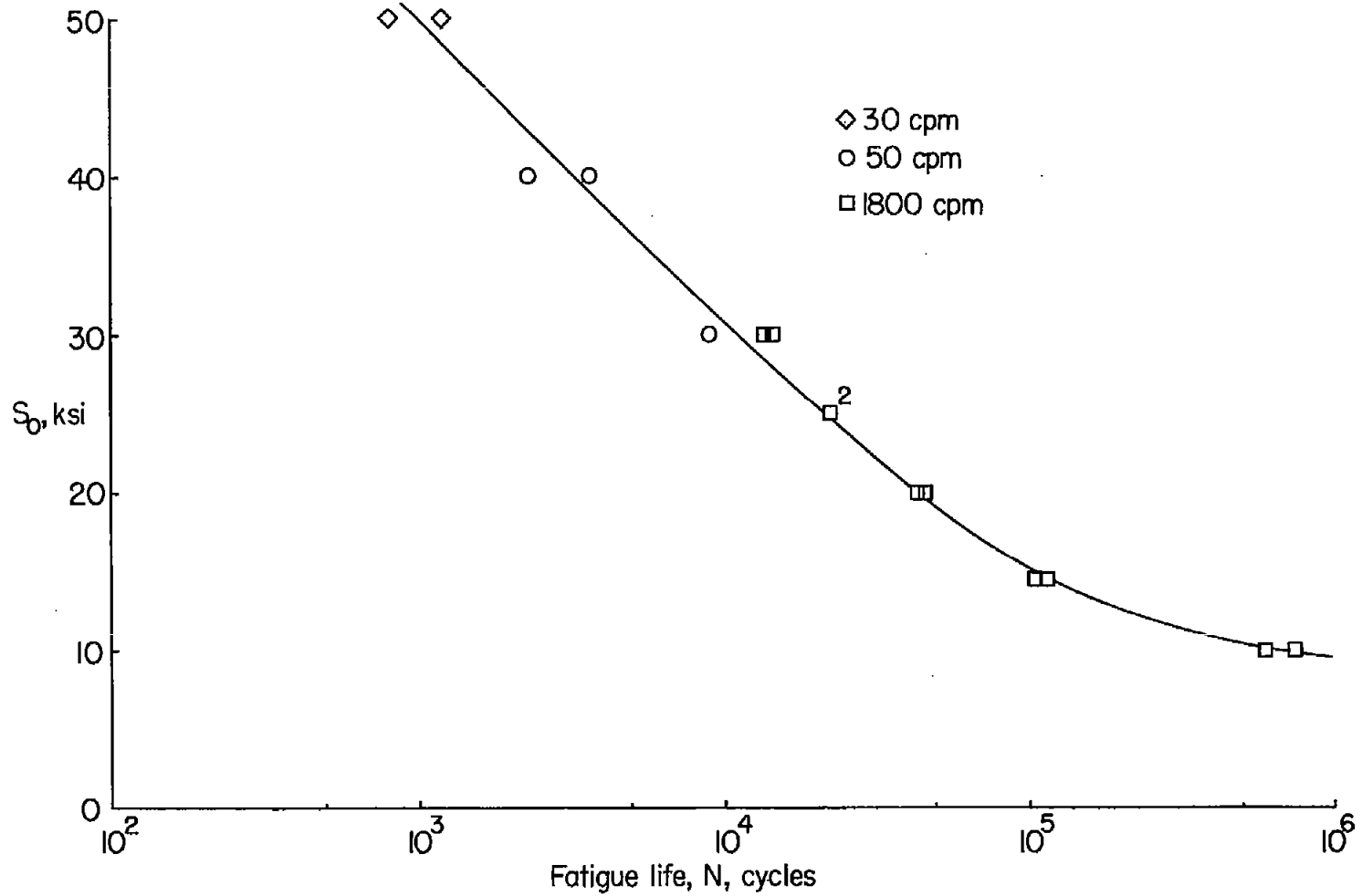


Figure 2.- Fatigue life of internally notched specimens of 2024-T3 aluminum alloy, 2 inches wide.
 $K_T = 7.4$.

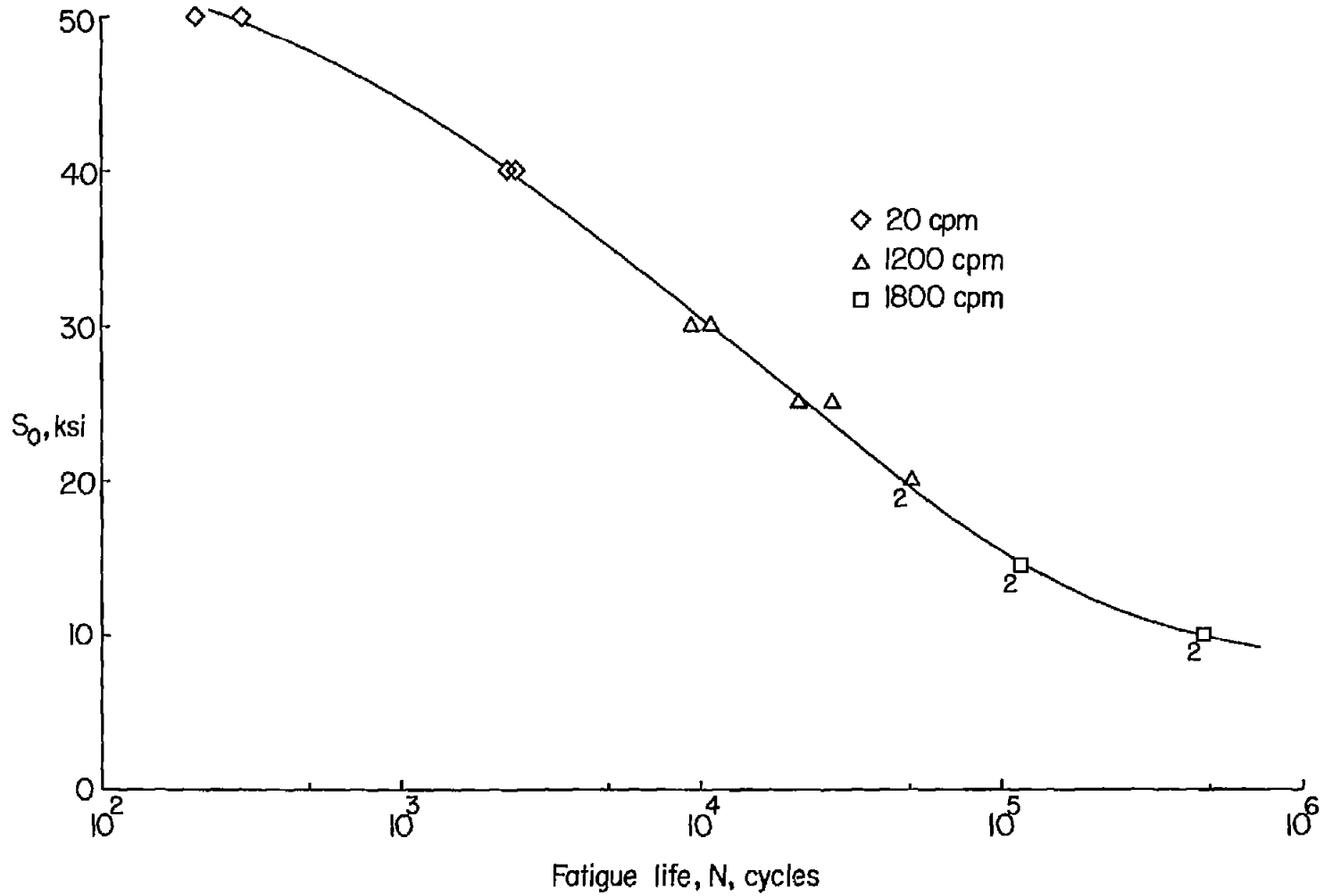


Figure 3.- Fatigue life of internally notched specimens of 2024-T3 aluminum alloy, 12 inches wide. $K_T = 7.9$.

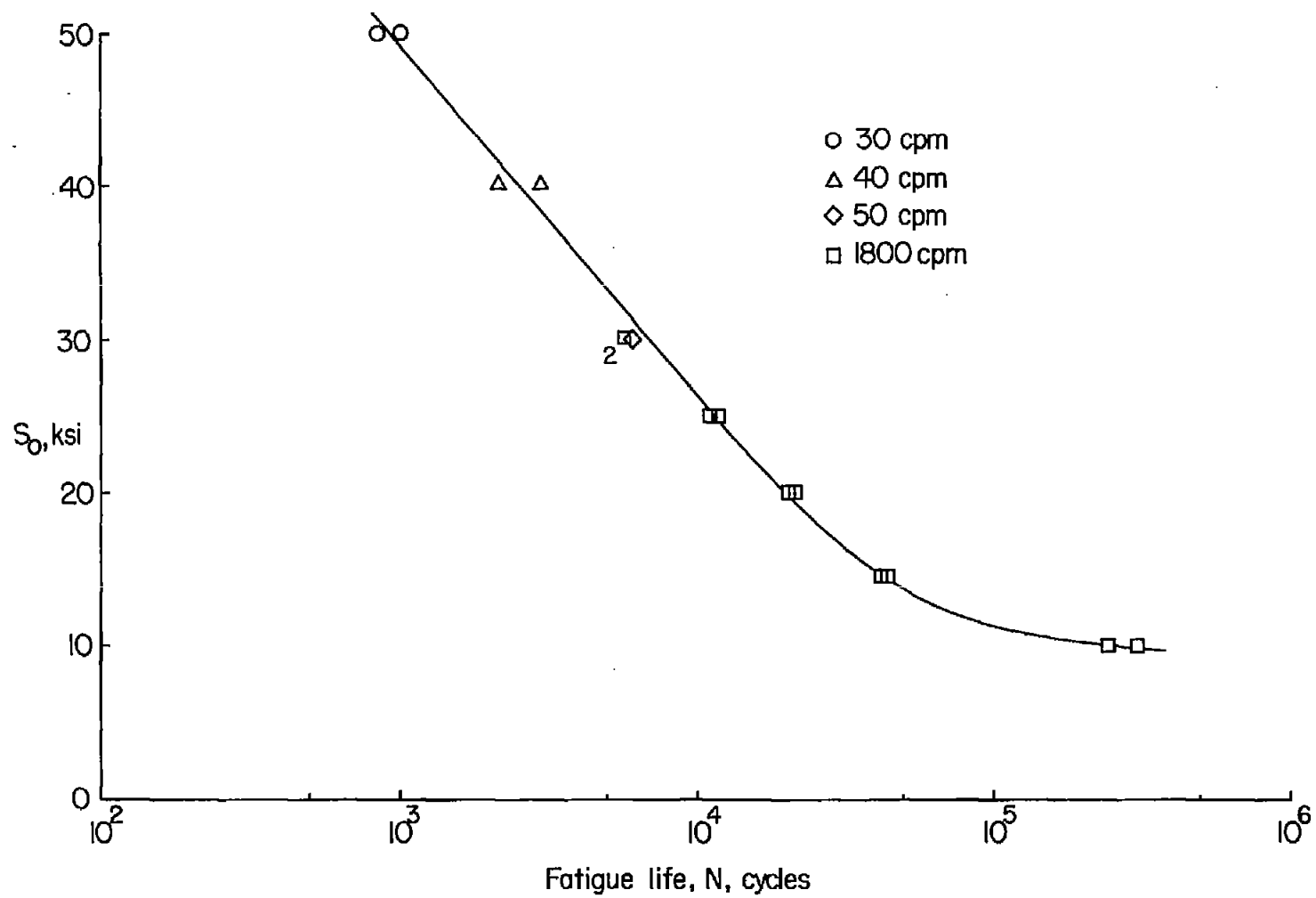


Figure 4.- Fatigue life of internally notched specimens of 7075-T6 aluminum alloy, 2 inches wide.
 $K_T = 7.4$.

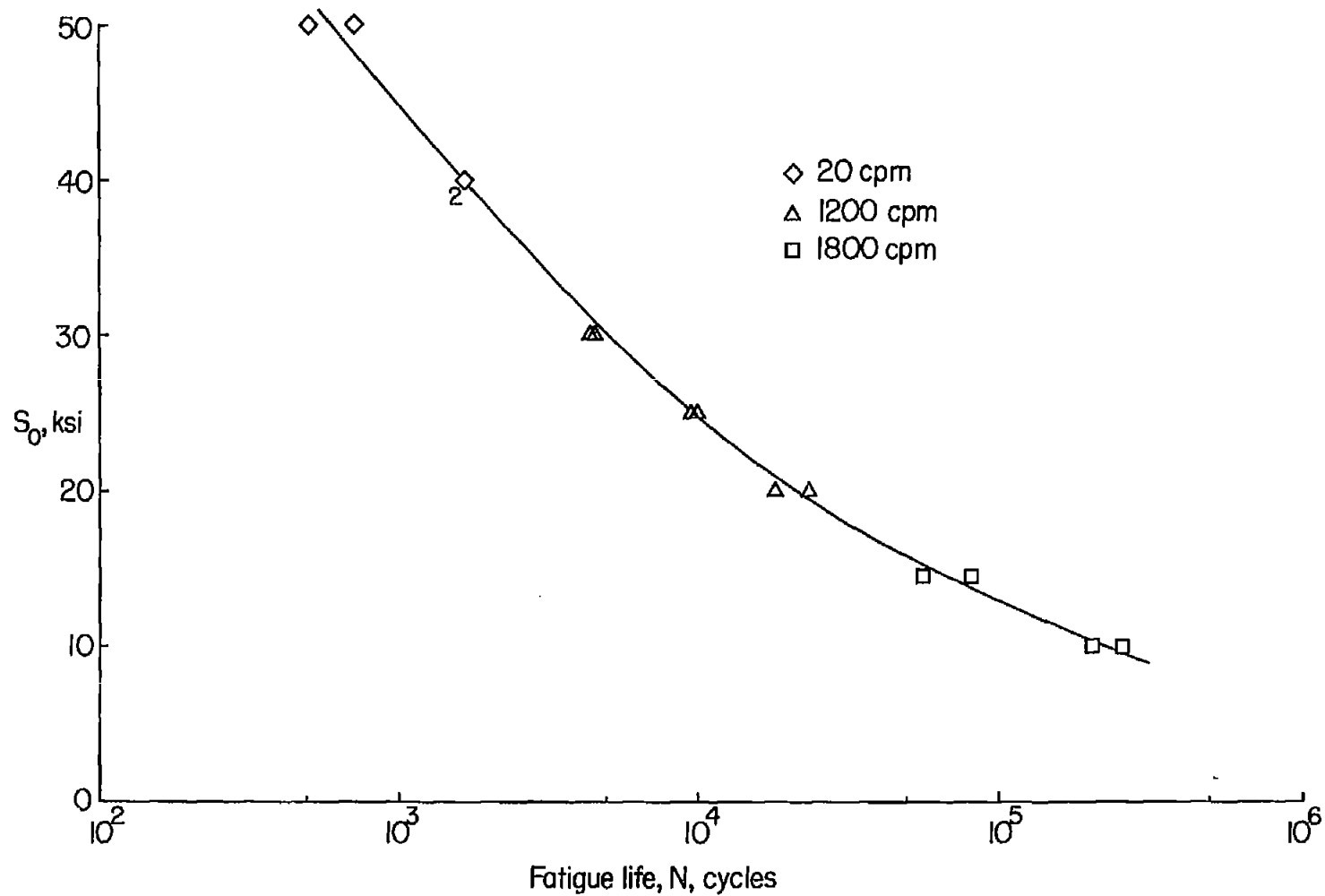
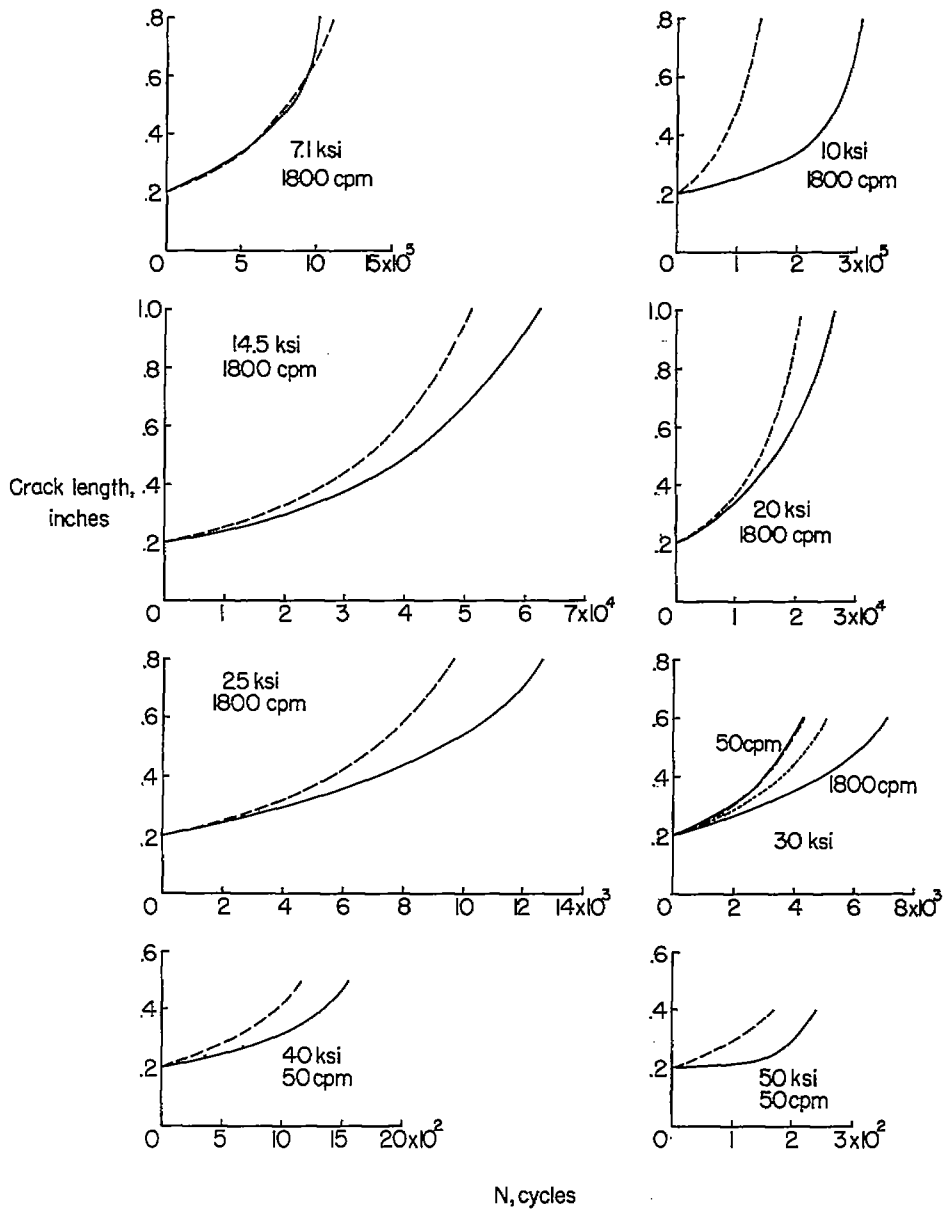


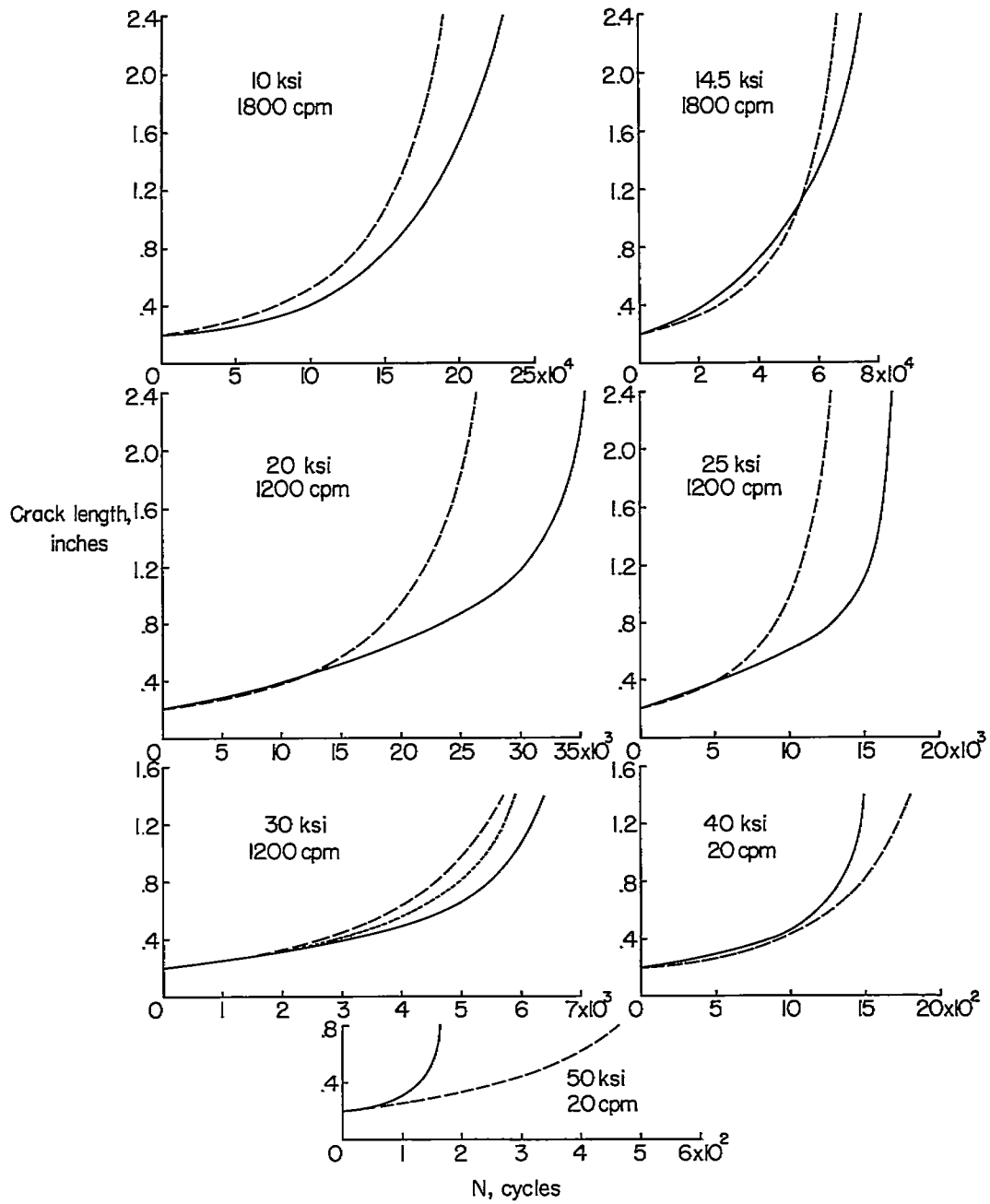
Figure 5.- Fatigue life of internally notched specimens of 7075-T6 aluminum alloy, 12 inches wide. $K_T = 7.9$.



(a) 2024-T3, 2 inches wide.

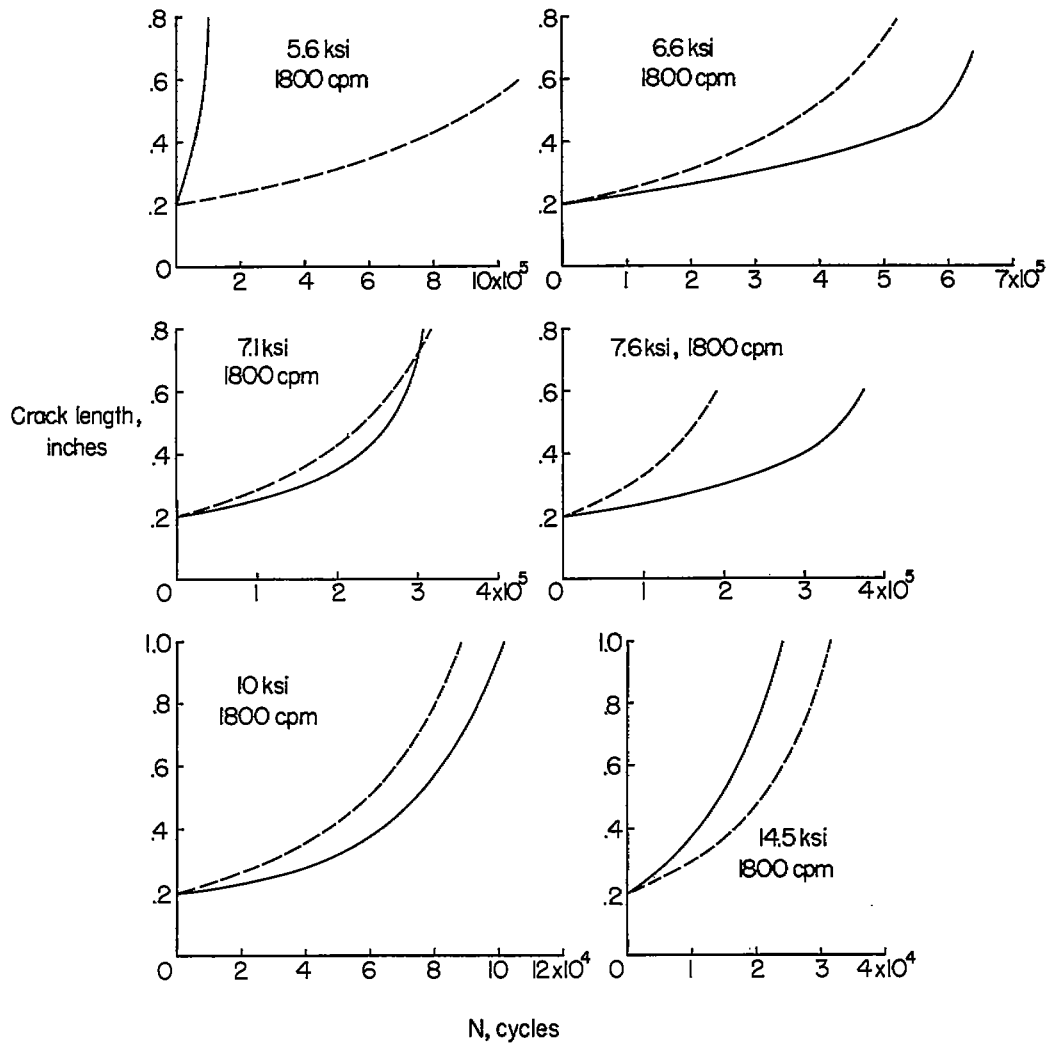
Figure 6.- Fatigue-crack propagation curves. Solid lines indicate experimental curves. Long-dashed lines indicate predictions by

$$N = C - \frac{1}{\alpha} \cdot x^{-\frac{1}{2}}$$
 Short-dashed lines indicate predictions by numerical integration.



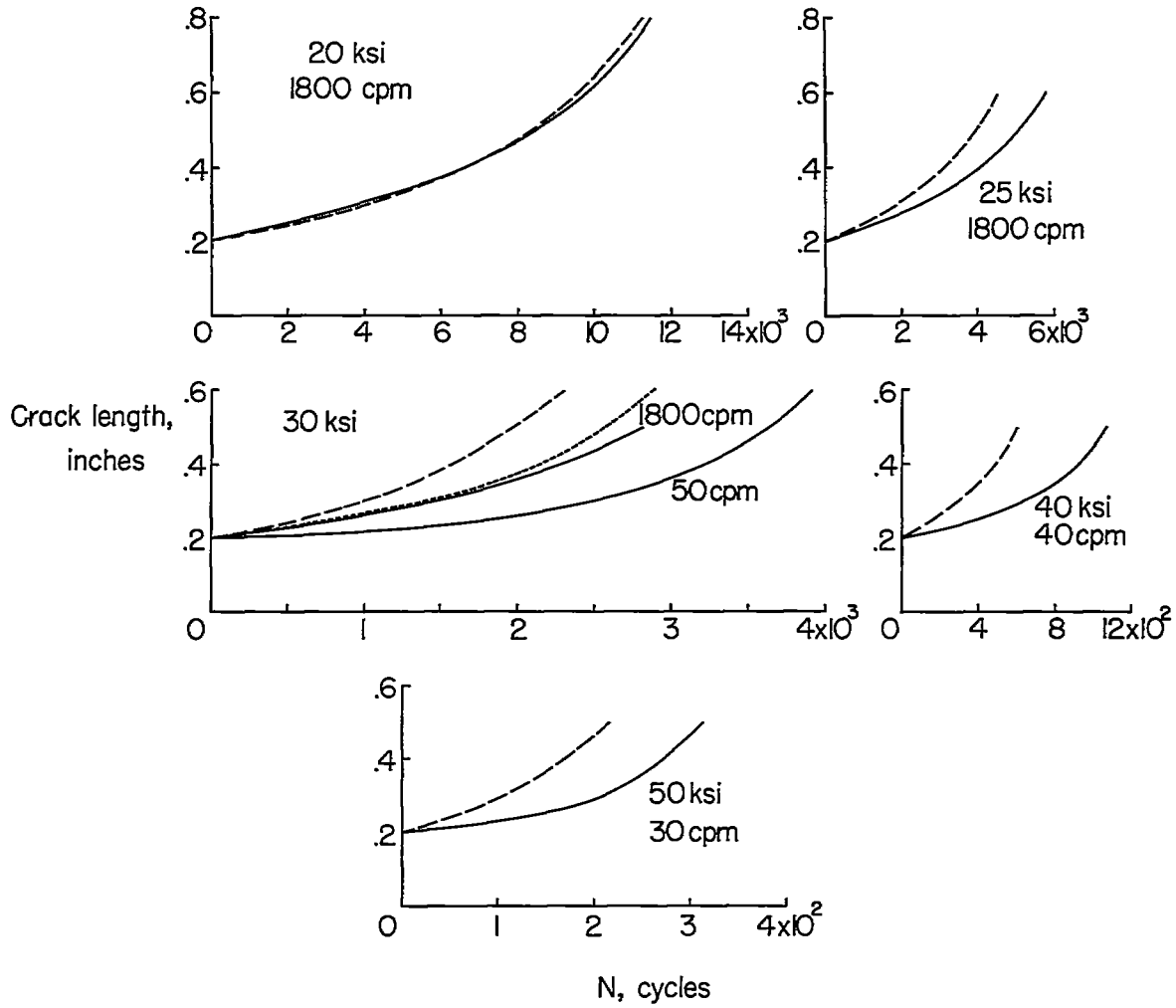
(b) 2024-T3, 12 inches wide.

Figure 6.- Continued.



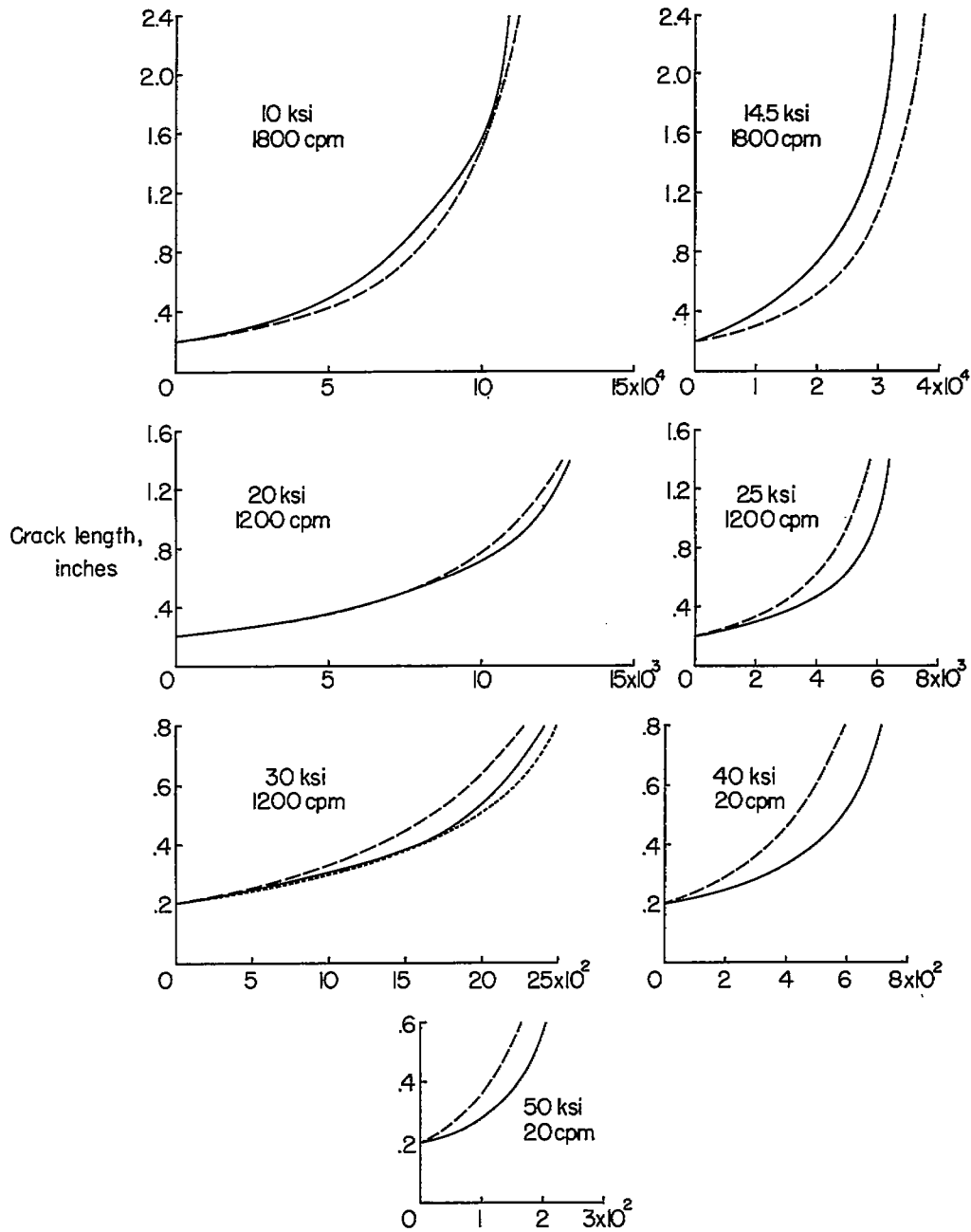
(c) 7075-T6, 2 inches wide.

Figure 6.- Continued.



(c) Concluded.

Figure 6.- Continued.



(d) 7075-T6, 1.2 inches wide.

Figure 6.- Concluded.

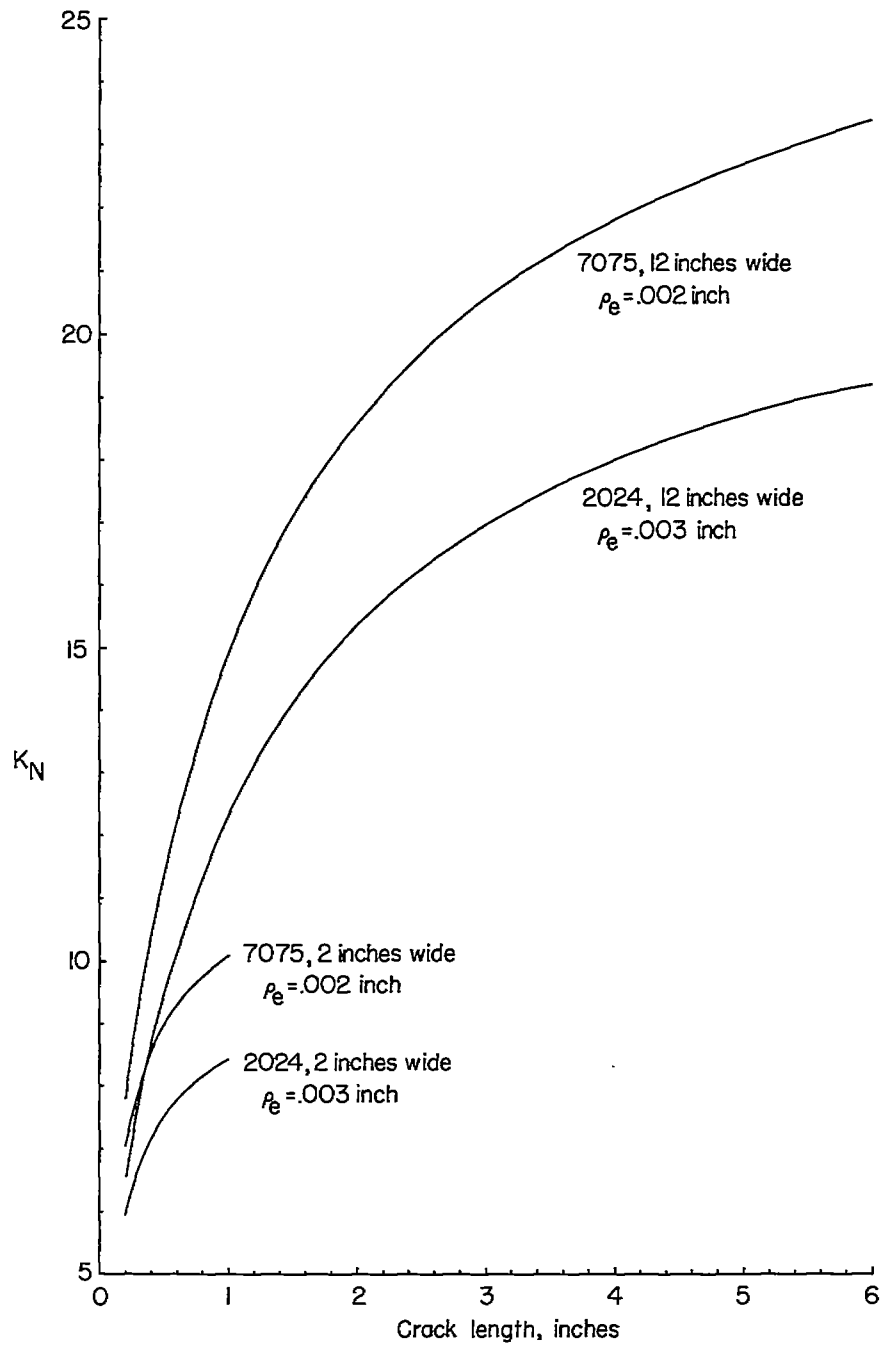


Figure 7.- Elastic stress-concentration factor for fatigue cracks corrected for size effect. 2024-T3 and 7075-T6 aluminum alloys.

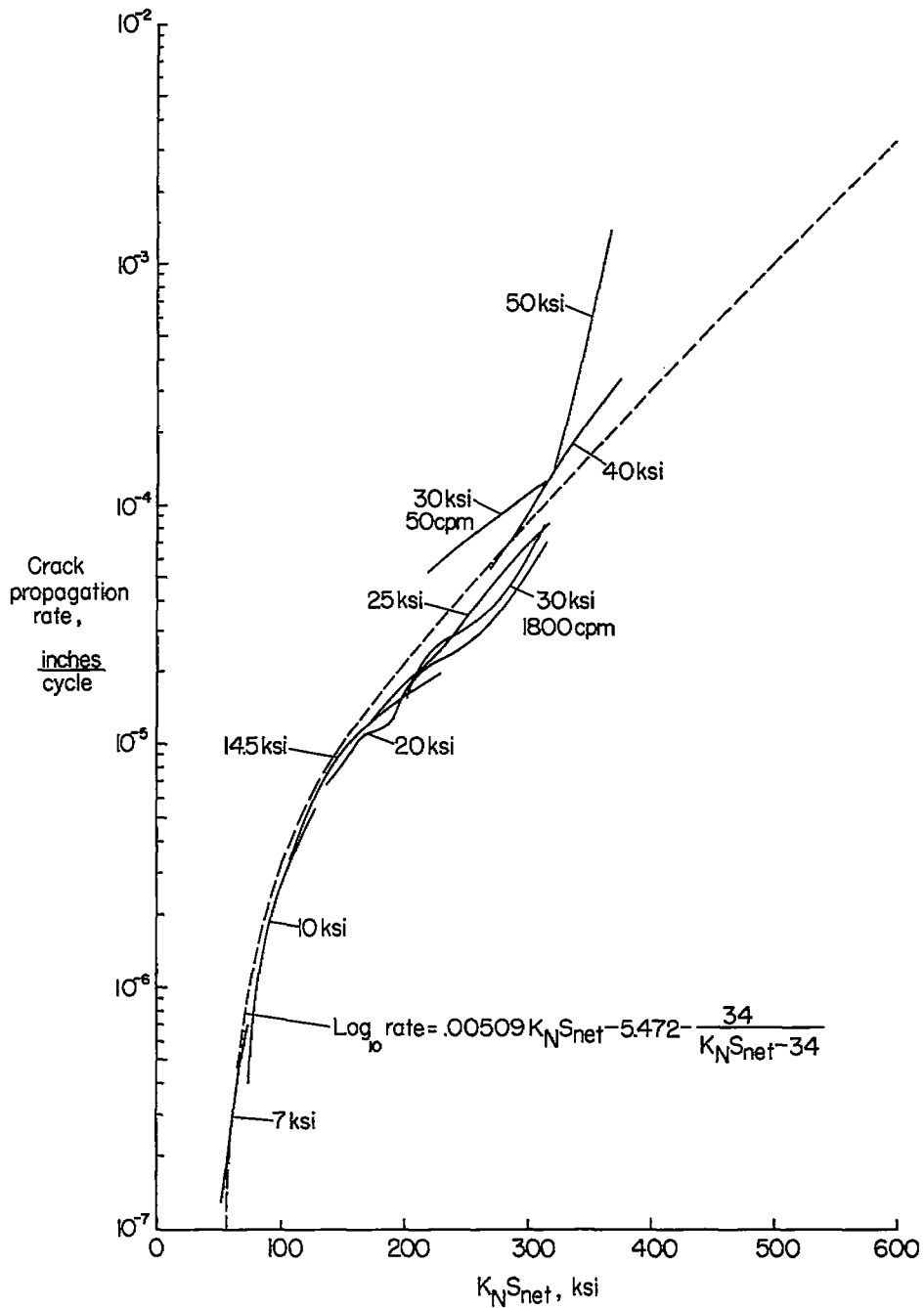


Figure 8.- Rates of fatigue-crack propagation in 2024-T3 aluminum-alloy sheet specimens, 2 inches wide. Stress values on curves indicate S_0 .

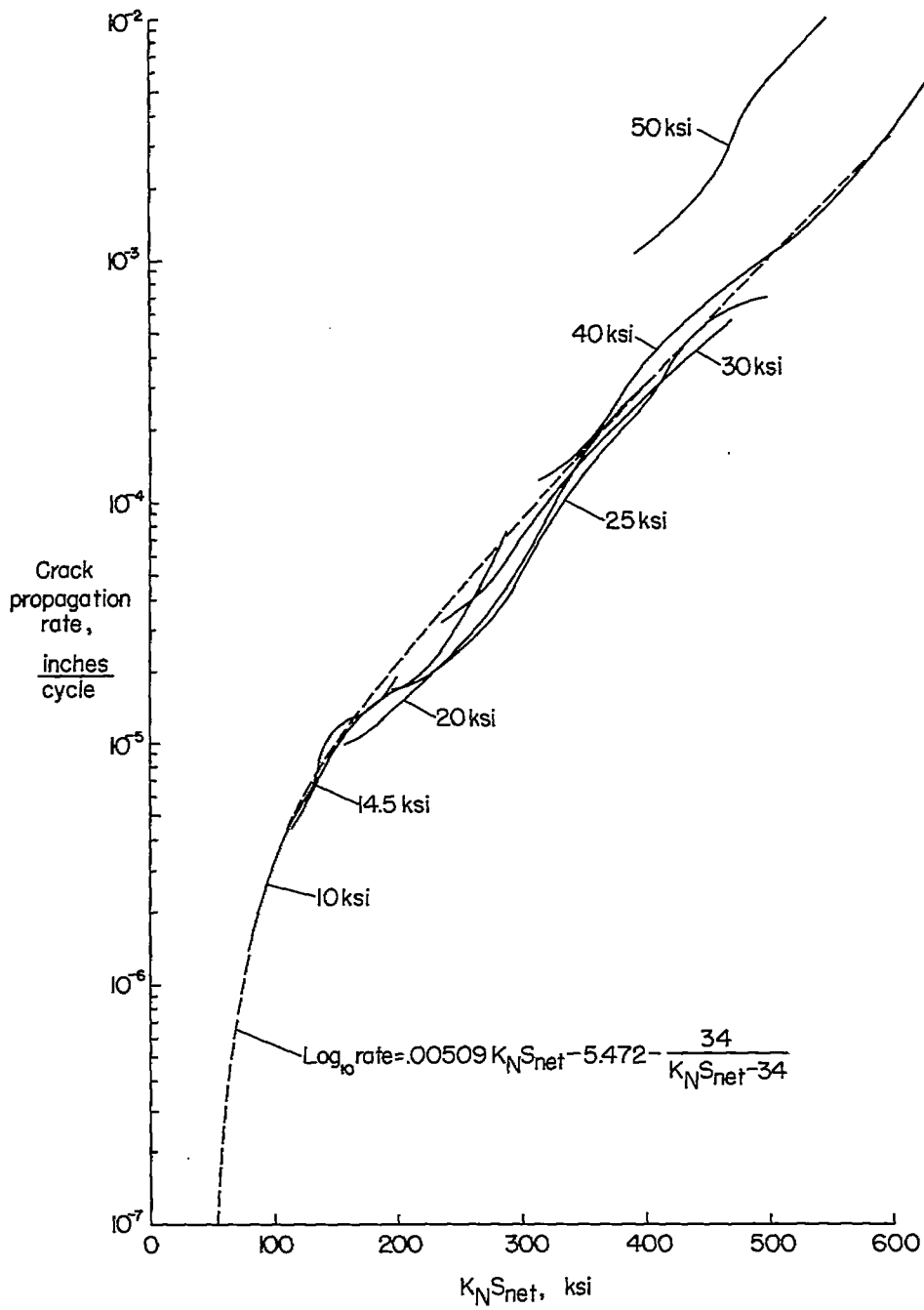


Figure 9.- Rates of fatigue-crack propagation in 2024-T3 aluminum-alloy sheet specimens, 12 inches wide. Stress values on curves indicate S_0 .

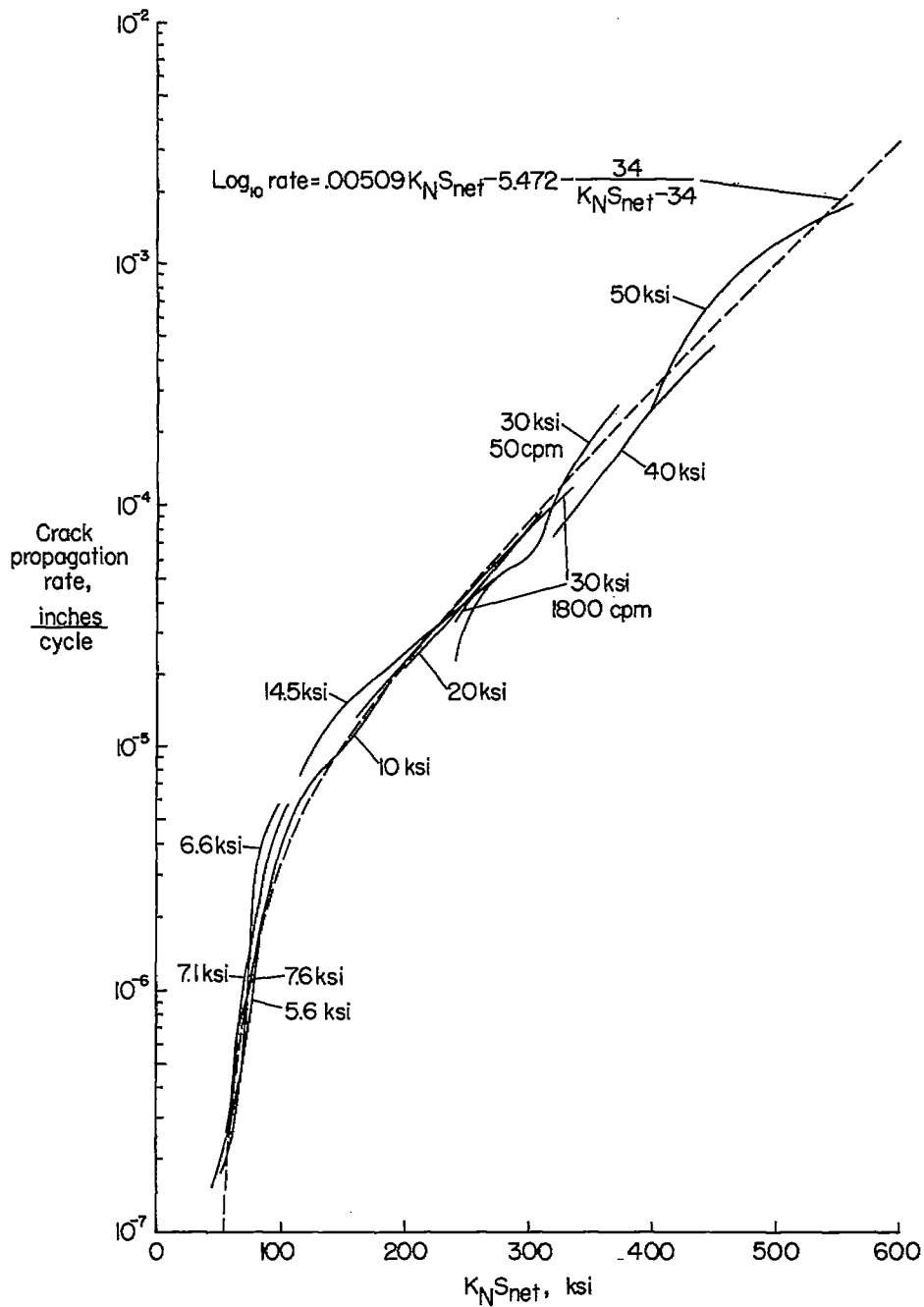


Figure 10.- Rates of fatigue-crack propagation in 7075-T6 aluminum-alloy sheet specimens, 2 inches wide. Stress values on curves indicate S_0 .

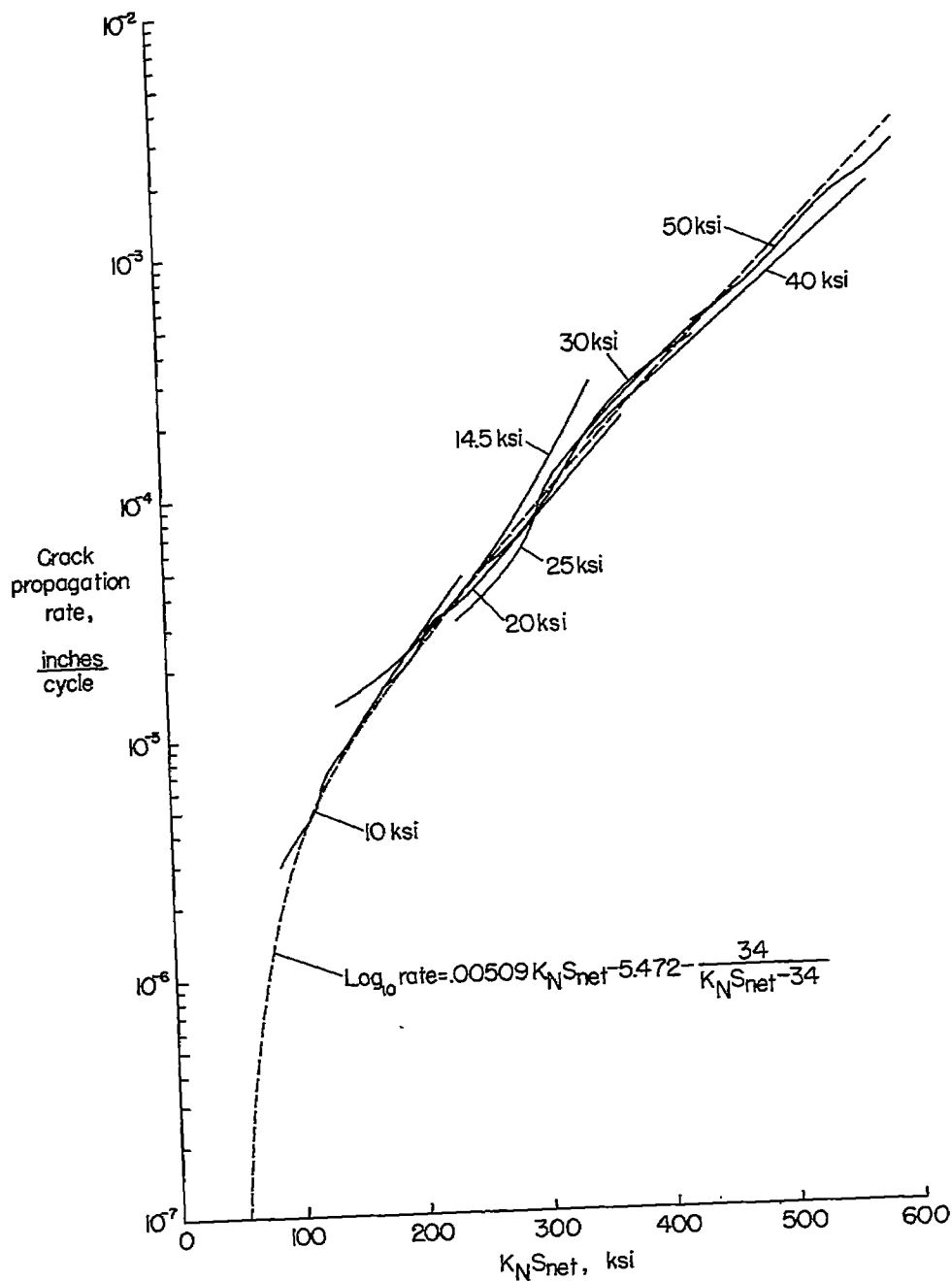


Figure 11.- Rates of fatigue-crack propagation in 7075-T6 aluminum-alloy sheet specimens, 12 inches wide. Stress values on curves indicate S_0 .

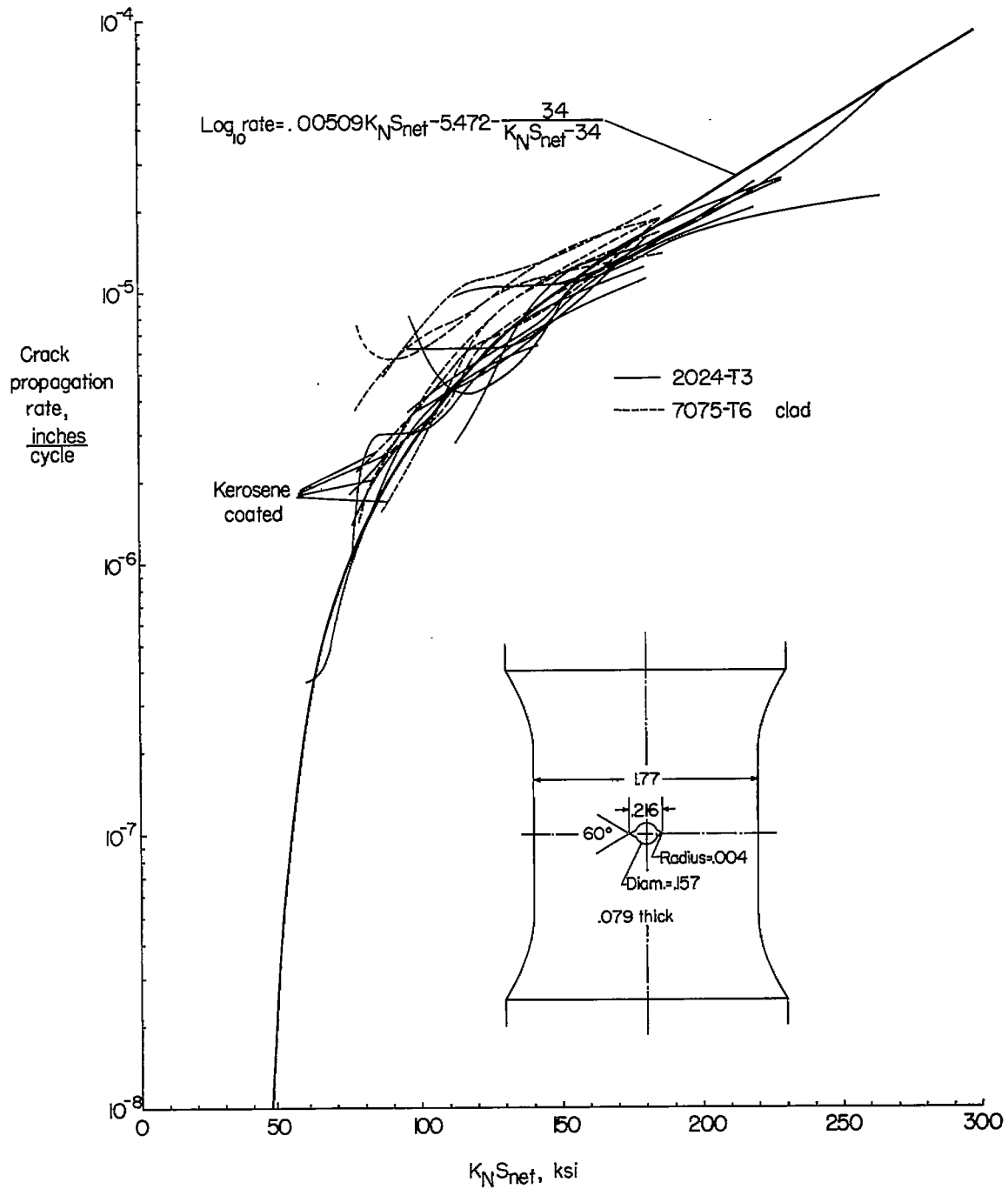


Figure 12.- Comparison of results of Weibull's constant-load tests (ref. 3) with rate expression of present paper (eq. (15)). Sketch indicates configuration of specimen tested by Weibull.

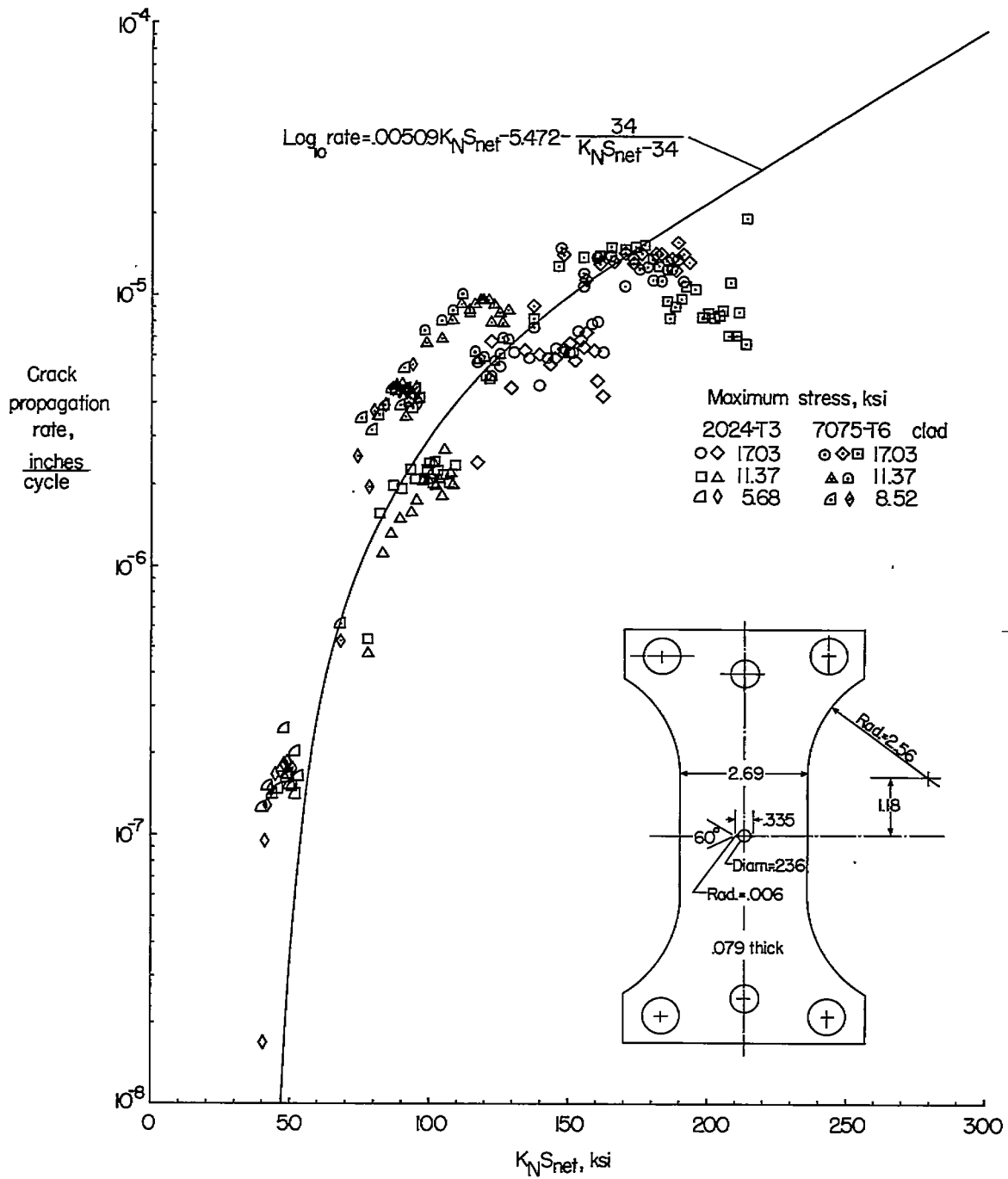


Figure 13.- Comparison of results of Weibull's constant-stress tests (ref. 4) with rate expression of present paper (eq. (15)). Sketch indicates configuration of specimen tested by Weibull.

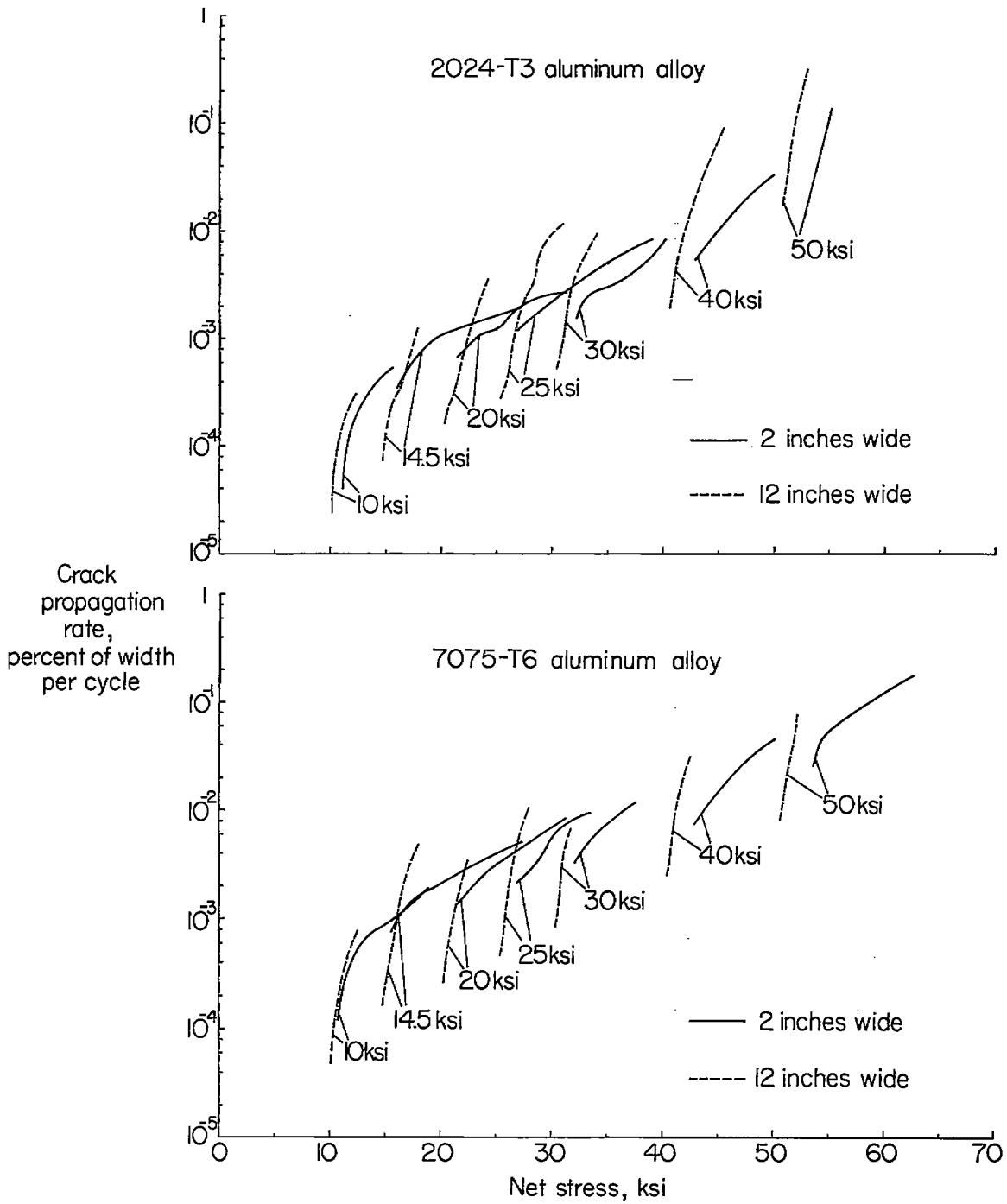


Figure 14.- Results of fatigue-crack-propagation tests. Stress values on curves indicate S_0 .

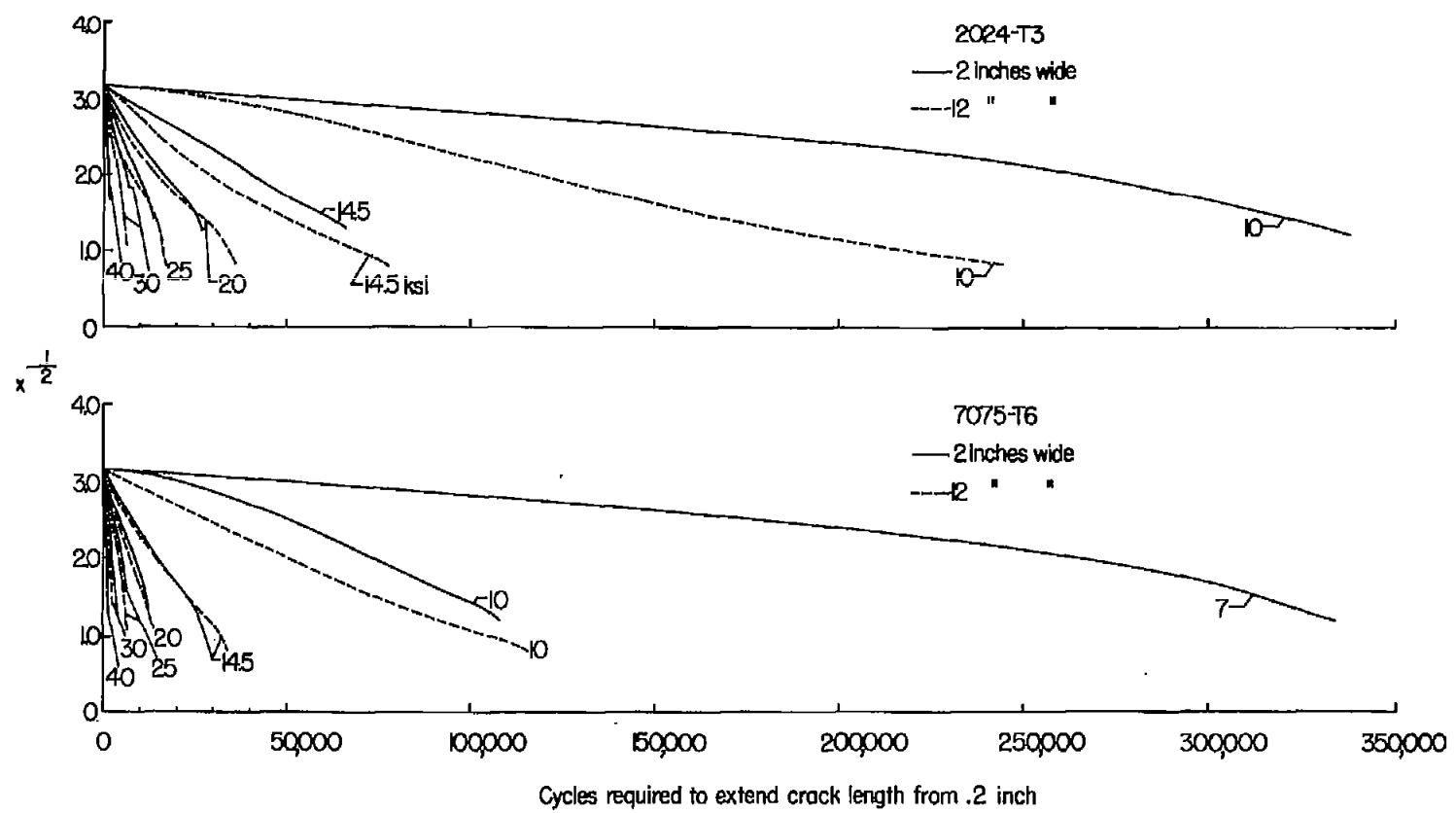


Figure 15.- Load cycles as a function of the reciprocal of the square root of one-half the crack length. Numbers on curves indicate S_0 .

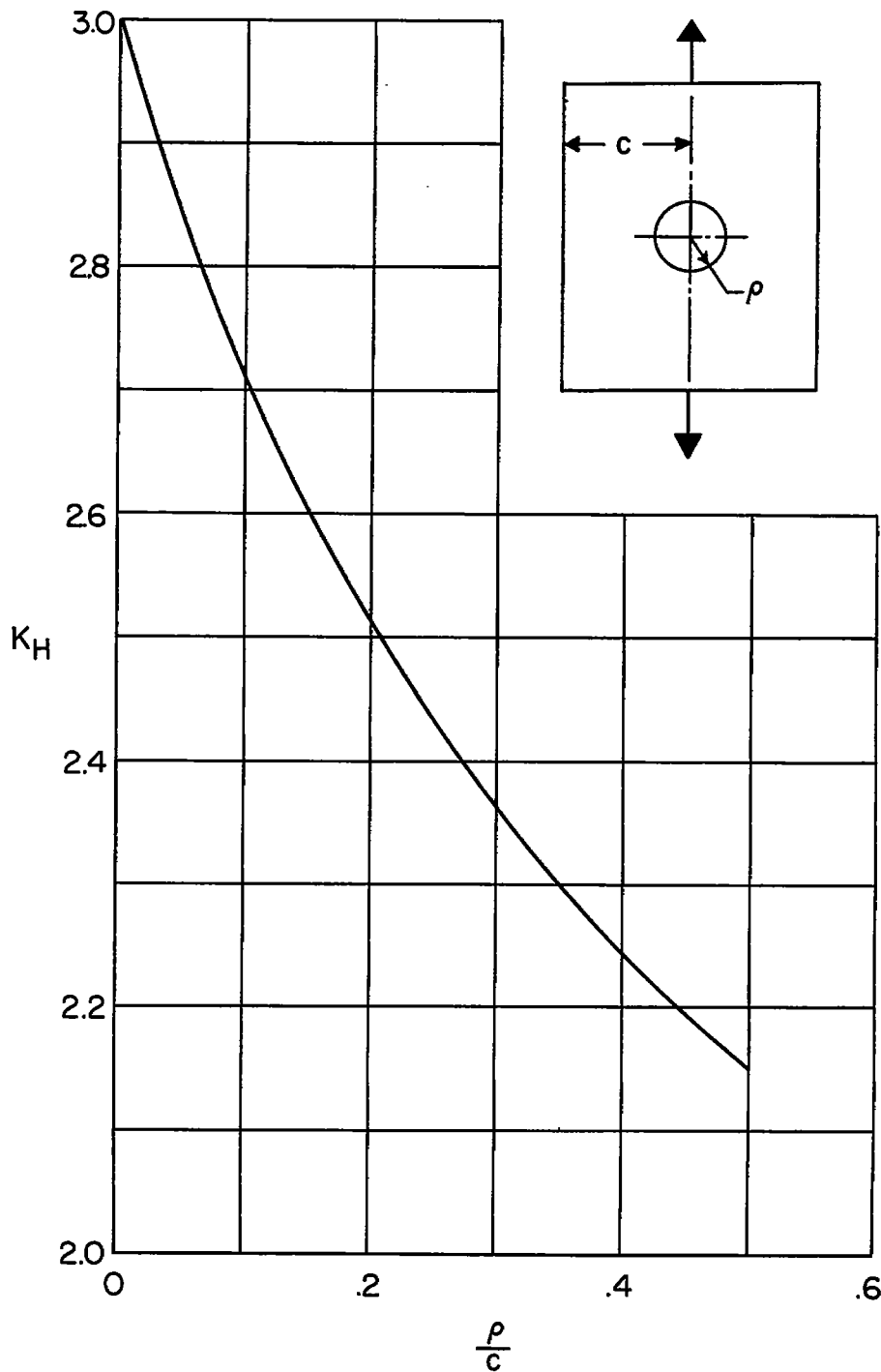


Figure 16.- Elastic stress-concentration factor for a circular hole in a finite sheet (ref. 11).